united nations educational, scientific and cultural organization

international atomic energy agency

the
abdus salam
international centre for theoretical physics

H4.SMR/1519-42

"Seventh Workshop on Non-Linear Dynamics and Earthquake Prediction"

29 September - 11 October 2003

Modelling of Block Structure Dynamics and Seismicity for Italian Area

A. Peresan[1], I. Vorobieva[3] , A. Soloviev[3], G.F. Panza[1, 2]

G.F. Panza

[1,] **Department of Earth Sciences**
University of Trieste

[2] **ICTP SAND GOUP, Trieste**

[3] **International Institute of Earthquake Prediction Theory and Mathematical Geophysics, Russian Academy of Sciences**
Moscow, Russia

MODELLING OF BLOCK STRUCTURE DYNAMICS AND SEISMICITY FOR ITALIAN AREA

A.Peresan, I.Vorobieva, A.Soloviev, G.Panza

Abstract

The block model of the lithosphere dynamics is used to simulate the active deformation and seismicity in the Italian region. The region . is represented as a system of rigid blocks, separated by infinitely thin fault planes, in viscoelastic interaction between themselves and with the underlying medium. The motion of the blocks is determined by the movement of the boundary blocks and of the underlying medium.

The results of the numerical simulation show that it is possible to reproduce the main observed features of tectonic motions. Particularly, the counter-clockwise rotation of Adria is obtained as a consequence of the Africa-Europe convergence and of the opening of the Tyrrhenian basin. The extensional zone along the Apennines and the compressional zone along the north-western boundary of the Adriatic Sea are correctly reproduced.

The synthetic and observed seismicity exhibit a pretty good agreement for the most seismically active areas. The slopes of the frequency-magnitude distribution for the synthetic and observed seismicity are close to each other.

The analysis of the source mechanisms of synthetic earthquakes shows a good agreement with the observations. Normal faulting is typical for Apennines, Eastern edge of Sicily and Calabrian arc, while reverse faulting has place in the north-western boundary of the Adriatic Sea, in Southern Alps and along Eastern edge of Adria along Dinarides.

1. Introduction

Seismicity is the manifestation of the complex nonlinear dynamics of the lithosphere, where earthquakes occur as a result of different processes, which are not entirely described and comprehended up to now. A possible approach to overcome the difficulties connected with the absence of fundamental constitutive equations and the impossibility of direct measurements at depth, where the earthquakes originate, relies on the integration of numerical modeling of the lithosphere dynamics and phenomenology of earthquake occurrence.

A number of dynamical models have been proposed to simulate seismicity, the most popular being the spring-slider block models proposed by Burridge and Knopoff (1967). Some models are "non-Earth specific" and reproduce only the very general features of seismicity, such as the frequency-magnitude relation. Some other try to simulate, at the cost of additional assumptions, further properties of the seismic sequences, like fluctuations in the activity and the space distribution of events (e.g. Yamashita and Knopoff, 1992). Each model tries to reproduce some peculiar properties of seismicity, based on different dynamical, kinematic or geometrical assumptions; nevertheless, no model can be expected to describe exactly the evolution of the Earth system, due to its complexity and possibly chaotic behavior.

The model of the lithosphere block structure dynamics, introduced by Gabriellov (1990), has, among the other models, an advantage consisting in its region-specificity: it allows to set up concrete driving tectonic forces, the geometry of blocks, and the rheology of fault zones. The model generates movement of blocks, comprising seismicity and slow movements (creep). The block model provides a straightforward tool for a broad range of problems: (i) connection of seismicity and geodynamics; (ii) dependence of seismicity on the general properties of f fault networks fragmentation; (iii) formulation and testing of different hypothesis for earthquake prediction purposes.

The model considers a seismic region as a system of blocks divided by infinitely thin plane faults. The blocks are assumed to be perfectly rigid. This assumption is argued for that in the lithosphere the effective elastic moduli of the fault zones are significantly smaller than ones within the blocks. The blocks interact between themselves and with the underlying medium and the interaction is viscoelastic. The system of blocks moves as a consequence of the motions prescribed for the boundary blocks and for the underlying medium. As the blocks are perfectly rigid, all deformation takes place in the fault zones and between the blocks and the underlying medium. The interaction of blocks along the fault zones is viscoelastic ("normal state"), until the ratio of the stress to the pressure remains below a certain strength level. When the critical strength level is exceeded in some part of a fault zone, a stress-drop ("failure") occurs. The modeling provides a synthetic earthquake catalogue, that reproduces some of the basic features of observed seismicity at regional scale: the Gutenberg-Richter law (e.g., Panza et al., 1997); the clustering of earthquakes (Maksimov and Soloviev, 1999); the dependence of the occurrence of large earthquakes on the fragmentation of the block structure and on the rotation of blocks (Keilis-Borok et al., 1997), etc. A detailed description of the model can be found in Soloviev and Ismail-Zadeh (2003).

The model enables to study relations between geometry of faults, block movements and earthquake flow, to reproduce regional features of seismicity, and to reconstruct tectonic driving forces from spatial distribution of seismicity.

The geometry of real faults and blocks was considered for several regions: Vrancea (Romania) earthquake-prone region (Panza et al., 1997) (Soloviev et al., 1999).; an effect of a sinking relic slab beneath Vrancea on the intermediate-depth seismicity was also studied by means of the block structure model (Ismail-Zadeh et al., 1999); Western Alps (Vorobieva et al., 2000; Soloviev and Ismail-Zadeh, 2003) were studied on the basis of the morphostructural scheme (Cisternas et al., 1985); Sunda Arc (Sunda Isles) (Soloviev and Ismail-Zadeh, 2003).

A set of numerical experiments performed adjusting the model parameters, permitted to obtain synthetic earthquake catalogs, which had a number of features similar to the observed seismicity. They include the locations of larger events, the direction of migration of earthquakes, the *b*-value of the FM plot, the source mechanism of the synthetic earthquakes, defined by the slip angles along the given faults (Soloviev et al., 2000).

The results of these experiments showed that this similarity may be used as a criterion to define, by a "trial-and-error" process, the range of parameters characterizing the tectonics of region. In particular, it seems possible to use the procedure of the block-structure dynamics modeling for the reconstruction of the direction of the tectonic motions in the region under study.

In this paper we consider a region covering Apennines peninsula and its neighborhood area. The block structure was outlined on the basis of the seismotectonic model developed by Meletti at al. (2000). The purpose of the study is to understand what features of seismicity of the region under consideration may be explained within the framework of this block structure and how the features of synthetic seismicity depend on variation of the movements specified in the model and other its parameters. As a continuation of this purpose we tried to reproduce main features of seismicity of the region under consideration and to find the model parameters, which are significant for this. We compare with the observed data the directions of the block motions obtained as a result of modeling and the following features of the synthetic seismicity: epicenter distribution, location of the strong events, type of the source mechanisms, the FM plot.

2. Brief Description of the Model

A block-structure is a limited and simply connected part of a layer, d, with thickness H bounded by two horizontal planes (Fig. 1). The lateral boundaries of the block-structure and its subdivision into blocks are formed by the portions of planes intersecting the layer called "fault planes". The intersection lines of the fault planes with the upper plane are called "the faults". The fault planes can have arbitrary dip angles which are specified on the basis of information on the deep structure of the region under consideration. A common point of two faults is called "the vertex". The vertices on the upper and the lower planes are connected by a segment ("rib") of the intersection line of the corresponding fault planes (see Fig. 1). The upper and the lower surfaces of the blocks are polygons. The lower surface of the block is called "the bottom". The fault structures seen in the upper and lower planes have the same topology.

The block-structure is bordered by a confining medium. The motion of the confining medium is defined in the continuous parts, delimited by two ribs of the block structure boundary, called "boundary blocks".

The blocks are assumed to be rigid, and all their relative displacements take place along the fault planes. The interaction of the blocks with the underlying medium take place along the lower plane, any kind of slip being possible. The fault planes and the bottoms of blocks are assumed to be infinitely thin viscous-elastic layers.

The movements of the boundary blocks and the underlying medium are assumed to be due to the external forces. The rates of these movements are assumed to be horizontal and known. The movement rates of the underlying medium can be different for each block.

Dimensionless time is used in the model. All variables containing time are referred to one unit of the dimensionless time, and the real time corresponding to the unit of the dimensionless time can be estimated during the interpretation of the results of the modeling.

Elastic forces arise in the lower plane and in the fault planes as a result of the displacement of the blocks relative to the underlying medium, to the lateral boundary, and to the other blocks. The elastic stress (the force per unit area) at a point is proportional to the difference between the relative displacement and the slippage (the inelastic displacement) at the point. The rate of the inelastic displacement is proportional to the elastic stress. Accordingly,

$$\mathbf{f} = K(\Delta\mathbf{r} - \delta\mathbf{r}), \quad \frac{d\delta\mathbf{r}}{dt} = W\mathbf{f}, \qquad (1)$$

where $\mathbf{f}$ is the vector of the elastic stress at the point of the lower plane or of the fault plane, $\Delta\mathbf{r}$ is the vector representing the relative displacement, and $\delta\mathbf{r}$ is the vector representing the inelastic displacement. If the fault plane is considered, then the coefficients K and W in (1) are, respectively, proportional to the shear modulus and inversely proportional to the viscous coefficient of the fault zone.

On the fault plane, the reaction force is normal to the fault plane and its size, per unit area, is:

$$|p_0| = |f_l \operatorname{tg} \alpha| \qquad (2)$$

where f_l is a component of the elastic stress, $\mathbf{f}$, normal to the fault on the upper plane, and α is the dip angle of the fault plane. The value of p_0 is positive in the case of extension and negative in the case of compression, respectively.

The state of the block structure is considered at the discrete time $t_i = t_0 + i\Delta t$ (i = 1, 2, ...), where t_0 is the initial time. At each time the translation vectors and the angles of rotation of the blocks are determined in such a way that the structure is in a quasi static equilibrium.

All displacements are supposed to be infinitely small, compared with the block size. Therefore the geometry of the block structure does not change during the simulation and the structure does not move as a whole.

The space discretization, that is necessary to carry out the numerical simulation of block structure dynamics, is made by splitting the surfaces, on which the forces act, into cells of trapezoidal shape and with linear size not exceeding a parameter ε. The coordinates X, Y, the relative displacement $\mathbf{\Delta r}$, the inelastic displacement $\delta\mathbf{r}$, and the elastic stress $\mathbf{f}$ are supposed to be the same for all the points of a cell.

The earthquakes are simulated in accordance with the dry friction model. For each cell of the fault planes, the quantity

$$\kappa = \frac{|\mathbf{f}|}{P - p_0} \tag{3}$$

is introduced, where $\mathbf{f}$ is the elastic stress given by (1), P is a parameter of the model which is assumed to be equal for all the faults. P can be interpreted as the difference between the lithostatic (due to gravity) and the hydrostatic pressure, which is assumed to be equal to 2 Kbars for all the faults, and p_0 is the reaction force per unit area, given by (2).

Three values of κ, $B > H_f \geq H_s$, are specified for each fault. It is assumed that the initial conditions - the translation vectors and the angles of rotation of the blocks and the inelastic displacements of the cells - for the numerical simulation satisfy the inequality $\kappa < B$ for all cells of the fault planes. If at any time in one or more cells the value of κ reaches or exceeds the level B, a failure ("earthquake") occurs.

The failure is defined as an abrupt change of the inelastic displacement $\delta\mathbf{r}$ in the cell. The new - after the failure - vector of the inelastic displacement $\delta\mathbf{r}^e$ is calculated from

$$\delta\mathbf{r}^e = \delta\mathbf{r} + \delta\mathbf{u}, \qquad \delta\mathbf{u} = \gamma\mathbf{f} \tag{4}$$

where $\delta\mathbf{r}$ and $\mathbf{f}$ are the inelastic displacement and the elastic stress, defined by (1), just before the failure and the coefficient γ is determined from the condition that the value of κ, after the failure, is reduced to the level H_f.

Once the new values of the inelastic displacements for all the failed cells are computed, the translation vectors and the angles of rotation of the blocks are determined to satisfy the condition of the quasi static equilibrium. If after these computations, for some cell(s) of the fault planes still $\kappa > B$, the procedure is repeated for this (these) cell(s), otherwise the numerical simulation is continued in the ordinary way.

On the same fault plane, the cells in which failure occurs at the same time form a single earthquake. The coordinates of the earthquake epicenter are determined as the weighted sum, with weights proportional to the areas of the failed cells, of the coordinates of the cells forming the earthquake. The magnitude of the earthquake is calculated from Utsu and Seki, (1954):

$$M = 0.98 \log_{10} S + 3.93 \tag{5}$$

where S is the total area of the cells forming the earthquake, measured in km^2.

For each earthquake, the source mechanism can be determined considering the vector $\mathbf{\Delta U}$, defined as the weighted sum, with weights proportional to the areas of the failed cells, of the vectors $\delta\mathbf{u}$, given by (4), for the cells forming the earthquake. From (4) and from the definition of $\mathbf{f}$ it follows that $\mathbf{\Delta U}$ lies in the fault plane where the earthquake occurs.

Immediately after the earthquake, it is assumed that the cells in which the failure occurred are in the creep state. It means that, for these cells, in equation (1), which describes the evolution of the inelastic displacement, the parameter W_s ($W_s > W$) is used instead of W. After the earthquake, the cell is in the creep state as long as $\kappa > H_s$, when $\kappa \leq H_s$, the cell returns to the normal state and henceforth the parameter W is used in (1) for this cell.

3. Geodynamics of the Region and the Block Structure under Consideration

As the initial step of the modeling the block structure should be outlined. There are two versions of the morphostructural zoning scheme of the region around the Adria margin, Apennines peninsular and Sicily (Caputo et al., 1980; Gorshkov et al., 2002). In principle these schemes may be assumed as a basis for the block structure of the region but the first one, made more than 20 years ago, requires to be updated using the new data about active faults, neotectonics and seismotectonics and the second was not completed when we started our study. At the same time it was rather interesting to try to use in this study the seismotectonic model of the region (Meletti at al., 2000).

According to Meletti et al. (1995, 2000), the recent geodynamics of the Central Mediterranean region is controlled by the Africa-Europe plate interaction and by the passive subduction of the south-western margin of the Adria plate. The main geological features observed in the Central Mediterranean area, on a regional scale, are represented by the Alps, by the back-arc Tyrrhenian extensional basin, by the Apennines and by the Padan-Adriatic-Ionic foreland. The Ortona-Roccamonfina line (Scandone et al., 1990) connects two major arcs in the Apennines chain corresponding to the Northern and Southern Apennines. The extensional rate that characterizes the southern part of the Tyrrhenian basin exceeds considerably those observed in the northern part. The boundary between these parts lies nearby the 41°N parallel and is associated with a discontinuity, marked by magnetic anomalies.

The western, northern and eastern boundaries of Adria are designated respectively by the Apennines, Alps and Dinarides, while the location of the southern boundary is controversial. A counter-clockwise rotation of Adria justifies the main characteristics, both structural and kinematics, of its boundary regions (Anderson and Jackson, 1987; Ward, 1994), such as the compressional front extending along the northeastern boundaries of the plate and its indentation in the Western Alps. Passing from east to west the structural features change: the Adria is subducting under the Eastern Alps and the Apennines, while in the Western Alps it is overthrusting on the European plate. Therefore the boundary between the Alps and the Apennines is a transform fault zone connecting the opposite lithospheric sinking. The evolution of the Apennines, however, does not seem to be explained by a simple convergence process and some evidences suggest that it may be controlled mainly by passive subduction processes.

The northern part of the Apennines peninsula is characterized by a band with tensional seismotectonic behavior, with prevailing dip-slip focal mechanism. Two belts run parallel to it: the western one is composed by the tensile zones near to the Tyrrhenian coast and the eastern one by the compressional zones along the Adriatic Sea. The model proposed by Meletti at al. (2000) for the deep structure of the Northern Apennines includes a connection at a depth between the Adriatic compressional front and the uplifting astenosphere along the Tyrrhenian Sea. This agrees with the geometry of the lithosphere-astenosphere system outlined by Calcagnile and Panza (1981), Della Vedova et al. (1991) and Marson et al. (1995) on the basis of the available data of relevant geophysical observations (surface waves, body waves tomography, heat flow, gravity).

The passive subduction of the Adriatic foreland in the Southern Apenninic Arc, from the Ortona-Roccamonfina line to the Taranto Gulf, seems to be ceased due to a detachment of the subducted slab, while it has continued in the Calabrian Arc. Corresponding to the concave part of the Calabrian Arc a zone of active seismicity is identified immerging toward the Tyrrhenian basin and reaching a depth of 500 km (Caputo et al., 1970, 1972; Anderson and Jackson, 1987).

It remains still undecided, is Adria connected to Africa plate or it moves as an independent plate. Up to now this is one of the most discussed questions. Neither a structural nor a seismically active boundary between Adria and Africa plate is evidenced (Panza, 1984).

At the same time the stress distribution appears compatible with a counter-clockwise rotation of Adria, with respect to Eurasia, whose rotation pole is well distinguished from that proposed for the Africa-Eurasia rotation. Therefore the movement of Africa plate appears different from the motion of its old promontory.

Summing the considerations given above we should note that the available information is not enough to define the block structure of the region by unique way. Taking as the basis the structural sketch shown in Figure 2 (Meletti et al., 2000) we outlined the block structure used for modeling dynamics and seismicity of the region. The configuration of its faults on the upper plane is presented in Figure 3. We tried to consider also the distribution of seismicity (Fig. 4) and the seismotectonic model of Scandone et al. (1994) in our structure of blocks and faults. It is rather natural because in the model earthquakes occur by definition only in fault planes. Therefore if we have a purpose to reproduce in the model the main features of the distribution of observed seismicity then the relevant faults have to be introduced in the structure.

The block structure (Fig. 3) consists of eleven blocks. These blocks are contoured by 36 faults. The point with the geographic coordinates 43.0^{o}N and 13.0^{o}E is chosen as the origin of the reference coordinate system. The X axis is the east-oriented parallel passing through the origin of the coordinate system. The Y axis is the north-oriented meridian passing through the origin of the coordinate system. The blocks and the faults composing the structure are marked in Figure 3 as I - XI and 1 - 36 respectively.

Two main discontinuities (faults 25 - 29) have been placed along Northern Apennines, to model the Adriatic compressional front and the extensional band. Fault 8 has been placed, corresponding to the Ortona-Roccamonfina line (Meletti et al., 2000), while faults 30 and 32 have been placed south of it to model the seismic activity from Irpinia to the Pollino, along the Southern Apennines. A possible discontinuity (fault 11) is assumed to exist between the Adria and Africa plate, south of Apulia; an almost EW oriented discontinuity (fault 33) has been placed according to the observed seismicity, crossing the Gargano and the Adria plate from the Apenninic chain up to the Dinarides.

To specify the motion of the confining medium at the lateral boundaries of the structure we introduce nine boundary blocks, which are marked as BB1 - BB9 in Figure 3.

To choose the value of thickness H of the layer d we analyzed the distribution of the hypocenters of observed seismicity. For the most part they are concentrated within 30 km. Another reason to specify H = 30 km is the new data on the dip structure of Central Mediterranean region. According to [??1] at an average depth of about 30 km there is a zone in the lithosphere where the velocity of the surface waves is rather low. It gives arguments to assume that it is a zone of heightened viscosity and therefore there is the decoupling at this depth between the upper and lower layers of the lithosphere.

The dip angles for the faults were specified on the basis of source mechanisms of observed earthquakes. The faults were separated into two groups: near-vertical and inclined faults. The same value of dip angle was specified for all faults from the same group: 85^o - for near-vertical faults and 60^o - for inclined faults. The dip angles of the faults are shown in Figure 3.

The heterogeneous geodynamics of the region under consideration requires to formulate an adequately complex block structure, hoping to be able to model a structure dynamic representative of the real one. Several parameters, describing its dynamical properties, must be defined for each block, hence the number of available observations about the real motion of the structures limits the detail of the model.

The results of recent geodynamical reconstruction for the central Mediterranean area have been considered, including GPS (Anzidei et al., 1996) and VLBI measurements (Ward, 1994) and paleomagnetic evidences (Sagnotti, 1992; Sagnotti et al., 1994; Aifa et al., 1988). This information has been used both to choose the prescribed velocities of the boundary blocks and underlying medium, and to evaluate the resulting motion of the blocks.

A problem that we encountered defining the model concerns the adequate representation of the opening of the Tyrrhenian basin and of the passive subduction, with the consequent flexure axis retreat, using a bidimensional system of absolutely rigid blocks. Practically, the opening is associated to displacements of blocks that can be obtained by means of a pulling force, applied by the boundary blocks; this representation, however, does not allow to model adequately the seismicity, since it would imply an unrealistic compression along the opening rim. The seismicity along the faults corresponding to the subduction zones can be described by means of a pushing force, but attention must be paid to its effect on the overall motion of the blocks.

A set of numerical experiments has been carried out. The values of the parameters of the blocks and the faults and movements specified for the underlying medium and the boundary blocks were varied in these experiments, and the following set of the values was assumed as a benchmark.

For all blocks and faults the coefficient in (1) are $K = 1$ bar/cm and $W = 0.05$ cm/bar.

For all faults the thresholds for κ are $B = 0.1$, $H_f = 0.085$, and $H_s = 0.07$, and the value of W in the creep state is $W_s = 5$ cm/bar.

The underlying medium for all blocks and boundary blocks BB1 - BB3 and BB6 - BB9 do not move. Boundary blocks BB4 and BB5 move progressively with the velocity V_x = -25 cm, V_y = 65 cm respectively. This direction was chosen accordingly to HS2-NUVEL1 model (Gripp and Gordon, 1990).

In all experiments the value of P in (3) equals 2 Kbars, and the values of the parameters for the discretization, in time and space, are respectively: $\Delta t = 0.0001$, $\varepsilon = 5$ km.

Below we call these values of the parameters as "standard set".

4. Numerical Experiments

Movements of the underlying medium and the boundary blocks were specified in the experiments taking into account the following main features of the geodynamics of the region:

- convergence of Africa and Europe;
- counterclockwise rotation of Adria with the pole in the Western Alps;
- opening of Tyrrhenian basin.

The following features of the observed seismicity, which follow from the analysis of the epicenter distribution and source mechanism, were used to estimate the results of the experiments on the basis of synthetic seismicity obtained in them:

- two belts in the Northern Apennines: the eastern one is compressional while the western one is extensional;
- double extensional belt in the Southern Apennines;
- compressional belts along the Dinarides and the Southern Alps
- absence of seismicity along southern boundary of structure, i.e. unknown boundary between Africa and Adria.

Below we give the description of the experiments.

Experiment 1

Purpose: to check, is it possible to explain main features of tectonic and seismicity in the region only by convergence of Africa and Europe.

Values of the parameters: the standard set given in Section 3.

Result. The counterclockwise rotation of the Adria is obtained, but the northern part of Adria (block IV) moves NW, but not N. The most of synthetic seismicity is concentrated along the southern boundary of the structure where observed seismicity is absent. Excluding two clusters of events in the Alps synthetic seismicity is absent in the northern part of the structure where there is a considerable part of observed seismicity. Displacements of the blocks are given in Table 1, epicenters of synthetic earthquakes are shown in Figure 5.

Experiment 2

Purpose: to check, how the results of modeling depend on the thickness of the structure.

Values of the parameters: the standard set with the value of H replaced by 15 km.

Result. Displacements of the blocks and the distribution of epicenters of synthetic earthquakes look like those obtained in Experiment 1, but synthetic seismicity in the Alps disappears. Level of seismic activity decreases. Displacements of the blocks are given in Table 2, epicenters of synthetic earthquakes are shown in Figure 6.

Experiment 3

Purpose: to remove synthetic seismicity from the southern boundary of the structure and to extend it the northern part of the block structure, to change the direction of motion of the Northern Adria.

Values of the parameters: the standard set with the following changes: the velocities of boundary block BB4 and the underlying medium for blocks IV - VIII and XI are chosen to simulate the rotation of Adria plate around the pole with geographical coordinates 44.2°N and 8.3°E (Meletti et al., 2000); the velocity of the underlying medium for block X are replaced by V_x = -25 cm, V_y = 65 cm (the same as the velocity of boundary block BB5).

Result. The counterclockwise rotation of the Adria is obtained, and the northern part of Adria (block IV) moves north. Extension along double faults 30, 32 in the Southern Apennines and compression along the Dinarides (faults 9, 10) are obtained. But the extensional – compressional belt in the Northern Apennines (faults 25 - 29) is not obtained. Synthetic seismicity is removed from the southern boundary of the structure and extends to the northern part of structure till Alps. High seismicity appears in the eastern edge of Sicily. The double seismic belt appears in the Southern Apennines, but there is no synthetic seismicity in the western edge of Northern Apennines. The level of seismicity is not high enough in the Calabrian arc and in Dinarides. Displacements of the blocks are given in Table 3, epicenters of synthetic earthquakes are shown in Figure 7.

Experiment 4

Purpose: to obtain the extensional – compressional belt in the Northern Apennines, to increase the level of seismic activity in the Calabrian arc.

Values of the parameters: the standard set with the changes made in Experiment 3 and the following additional changes: the velocities of boundary block BB7 and the underlying medium for block III are replaced respectively by V_x = -30 cm, V_y = 30 cm, and by V_x = 55 cm, V_y = 45 cm.

Result. The counterclockwise rotation of the Adria is obtained, extension in the Southern Apennines and compression along the Dinarides are obtained. The extensional – compressional belt in the Northern Apennines is also obtained. Synthetic seismicity appears in the western edge of the Northern Apennines but its level is too high. Synthetic seismicity increases in the Calabrian arc and is too high in the eastern edge of Sicily. Displacements of the blocks are given in Table 4, epicenters of synthetic earthquakes are shown in Figure 8.

Experiment 5

Purpose: to analyze, how synthetic seismicity depends on the coupling of the blocks with the underlying medium.

Values of the parameters: the standard set with the changes made in Experiment 4 and the following additional changes: for blocks I, III, V, VII, and XI the value of W is replaced by 0.005 cm/bar; for block II the value of W is replaced by 0.015 cm/bar

Result. There are no great changes in seismicity comparing with experiment 4. The level of synthetic seismicity increases slightly in the compressional belt of Northern Apennines and remains too high in the western edge of Sicily and in the extensional belt of Northern Apennines. Displacements of the blocks are given in Table 5, epicenters of synthetic earthquakes are shown in Figure 9.

Experiment 6

Purpose: to decrease the level of synthetic seismicity in the extensional belt of the Northern Apennines and in the eastern edge of Sicily and to increase synthetic seismicity in the compressional belt of Northern Apennines.

Values of the parameters: the standard set with the changes made in Experiment 5 and the following additional changes: for faults 25 - 27 (the eastern edge of the Northern Apennines) the values of W and W_S are replaced respectively by 0.005 and 0.5 cm/bar, and for faults 15, 28, and 29 (the eastern edge of Sicily and the western edge of Northern Apennines) the values of W and W_S are replaced respectively by 0.5 and 50 cm/bar.

Result. The level of synthetic seismicity decreases in the western edge of the Northern Apennines and in the eastern edge of Sicily and increases in the Southern Apennines. Displacements of the blocks are given in Table 6, epicenters of synthetic earthquakes are shown in Figure 10.

5. Discussion

In the experiments described above we varied the following parameters: the velocities of the boundary blocks and the underlying medium and the coefficients defining visco-elastic characteristics of the faults and the block bottoms, which control the portion of the elastic energy released through earthquakes and the coupling of the blocks with the underlying medium. Curing out the experiments we changed the parameters trying to reproduce the main features of observed seismicity and of the geodynamics of the region.

In the first experiment, when the movement of the boundary blocks representing Africa plate is only specified, it is impossible (within the framework of the model) to obtain the directions of the block motions and the distribution of synthetic epicenters like those known from the observations. Decreasing of the thickness of the structure made in the second experiment results in more difference between synthetic and observed seismicity.

In the third experiment we try to introduce the rotation of Adria plate around pole placed in the Western Alps (Meletti et al., 2000). As a result the movements of the blocks and synthetic seismicity becomes more similar to the observations than in the first experiment.

The fourth experiment is based on the assumption that opening of the Tyrrhenian basin is an independent phenomenon, which influences to the region and, in particular may explain the compressional - extensional belt in the Northern part of Apennines. We model opening of the Tyrrhenian by specifying the movement of the underlying medium for block III (the Northern Apennines) with the velocity in the NE direction, that allows to obtain extension in the western edge of the Apennines and compression in the eastern edge. One may interpret this as taking into account the rising mantle flow, which causes the complex structure in the Northern Apennines. Specifying the movement of boundary block BB7 we model opening Tyrrhenian basin in its southern part; that may cause the increasing of synthetic seismicity in the Calabrian arc. As a result the tectonic motions are reproduced in the model more accurately, and likeness between distributions of synthetic and observed epicenters is improved considerably. But the comparative levels of synthetic seismicity for different parts of structure are not in sufficient consent with the observations.

In the fifth experiment we change the coefficients defining visco-elastic characteristics of the block bottoms in the Calabria Apennines and the Alps. We decrease for these block bottoms the value of W - the rate of growth of the inelastic displacements in the block bottoms. This makes more hard connection between these block bottoms and the underlying medium and reflects coupling along the Apennines Alps and in Calabria. Coupling provides more effective transmission of the motion of the underlying medium to the blocks of the structure. As a result of this experiment synthetic seismicity increases in the compressional belt of the Northern Apennines and in the Southern Apennines.

In the sixth experiment we change the parameters defining visco-elastic characteristics of the faults along the eastern edge of Sicily and the western edge of the Northern Apennines. The level of synthetic seismicity obtained in these faults in the fifth experiment is too high. The corresponding zones are extensional and we assume that the Earth crust here is possibly softer and more plastic than in another parts of the region. If it is so, then the considerable part of stress may release through creep without earthquakes. We increase parameters W and W_s controlling the rate of increase of inelastic displacements that may decrease the level of synthetic seismicity in these faults. We decrease also W and W_s for the faults along the eastern edge of the Northern Apennines. Redistribution of the stress in the block structure may cause the appearance of synthetic seismicity in another faults. As a result the synthetic seismicity in the western edge of the Northern Apennines and in the eastern edge of Sicily decreases.

We consider that in the sixth variant the model reproduces the tectonic motions in the region under consideration, and some features of observed seismicity, mainly the epicenter distribution and the levels of seismicity in different parts of the region. Below we discuss in detail the results obtained in this variant.

Block movements

The numerical simulation of the block structure dynamics has been performed for a period of 20 units of dimensionless time. The resulting displacements of the blocks are shown in Figure 11; the exact values of the translational and rotational displacements for the blocks are given in Table 6.

All the blocks move in the NE direction, except blocks I and X, which represent Western Alps and Sicily and move in the NW direction. The absolute values of displacement decrease going northward, and blocks I and II representing the Alps are almost immovable; this might be explained to some extent, by a predominance of vertical motions (Gubler et al., 1981; Geiger et al., 1986), which cannot be reproduced by the model. The counter-clockwise rotation of blocks IV and VI is in a good agreement with the rotation of the Adria plate (Meletti et al., 2000). Comparing the resulting displacements of the blocks (Table 6 and Fig. 11) it is possible to observe that there is extension on faults 28, 29 30 and 32, which represents the extension zone along the Apennines, and compression at the eastern edge of block III, which represents the compressional band along the Adriatic Sea in the Northern Apennines. The compressional zones are formed along the eastern edge of blocks IV and VI (the boundary between the Adria plate and the Dinarides), and along the southern boundary of the Alps (fault 24), while an extensional zone is obtained in the Calabrian Arc (faults 19 and 20 in Fig. 3).

Synthetic seismicity

The distribution of the epicenters of the synthetic earthquakes is shown in Figure 10. The magnitude range of the synthetic earthquakes is between 5.2, which is the minimum magnitude, allowed by the specified value of ε (5 km), and 7.6.

There is a rather good agreement between the distributions of synthetic (Fig. 10) and observed (Fig. 4) epicenters. The observed seismicity is presented by the available historical data of Leydecker (2001) and the catalogues CCI+NEIC for the period 1000-2000 (Peresan et al., 2000). Below we compare synthetic and observed seismicity in the specific areas with the high level of observed seismicity.

The Northern Apennines (faults 25, 26, 27, 28, and 29). Synthetic seismicity presents two belts here. The western one is more active than the eastern that agrees with the observations. The largest synthetic events (with $M = 6.8$) are obtained near the conjunction of the Apennines and the Alps, where the level of the observed seismicity is not too high.

The Southern Apennines (faults 30 and 32). Synthetic seismicity also present two belts here, the level of synthetic seismicity is higher then in Northern Apennines, that is in agreement with observations. The maximum magnitude of synthetic events equals 7.6. Here the largest observed earthquakes occurred in 1930 (M = 7.45) and 1857 (M = 7.0) and several events with $M \geq 6.5$ are also reported.

The Calabrian arc (faults 19 and 20). The level of synthetic seismicity is high here, the maximum magnitude is 7.3. The largest observed earthquake (Messina, 1908) has M = 7.1.

The eastern edge of Adria (faults 9 and 10). The level of synthetic seismicity is not high enough in the southern part of Dinarides, maximum magnitude is 6.8 here, while the observed maximum is 7.5. The area of the highest synthetic seismicity is obtained in the Northern Dinarides, several synthetic earthquakes with magnitude $M \geq 7.5$ occur here, for the largest one M = 7.6. The maximum observed magnitude here is also 7.9 (in 1348) the event occurred in the vicinity of the conjunction of the Alps and the Dinarides.

The eastern edge of Sicily (fault 15). Maximum magnitude of synthetic earthquakes obtained here is 7.2. The largest observed earthquake with M = 7.5 occurred along the Malta escarpment in 1693 and several events with $M \geq 6.5$ are also reported here.

The Southern Alps (fault 24). Maximum magnitude of synthetic earthquakes obtained here is .6.6. The largest observed earthquake M = 6.8 occurred in the central part of the Southern Alps in 1222. The level of synthetic seismicity is in agreement with the observations.

The slope (b-value) of the frequency-magnitude (FM) plot (Fig. 12) appears larger for the synthetic seismicity (1.44) than for the observed one (1.14).

Source mechanisms

The source mechanisms of the synthetic earthquakes have been analyzed for different parts of the structure. The mechanism of an earthquake can be described by means of three angles: strike, dip, and slip. Strike and dip define the azimuth and the dip angle of the rupture plane, while slip defines the direction of the displacement along the rupture plane. In the block model, strike and dip are prescribed by the block structure geometry, the only free parameter is slip. The values of slip have the following meaning: 90° and -90° correspond respectively to normal and reverse faulting, 0° and 180° indicate respectively right-lateral or left-lateral strike-slip mechanism.

The source mechanisms of the observed earthquakes (e.g., Saraò et al., 1997) are shown in Figure 13.

For the Northern Apennines (faults 28, 29) and Southern Apennines (faults 30, 32) the histograms of the slip values obtained for synthetic earthquakes is given in Figures 14 and 15. One may observe that the maximum in the histogram is nearby 90°, varying from 70° to 110°. Hence most of the synthetic earthquakes correspond to normal faulting.

The similar histogram for the western margin of the Adria plate, along the Northern Apennines (faults 25 and 26) is given in Figure 16. Here the maximum is nearby -120° that corresponds to reverse faulting. Nevertheless, a certain part of the synthetic earthquakes is characterized by normal faulting and strike-slip.

For the Southern Alps (fault 24) the maximum in the histogram is between -105° and -85° (Fig. 17) that corresponds to reverse faulting.

The most of the synthetic earthquakes obtained for the Calabrian Arc (faults 19 and 20) show normal faulting, with the maximum in the histogram of the slip values being between 80° and 120° (Fig. 18).

The slip values of the synthetic earthquakes obtained for the eastern edge of Sicily (fault 15) are concentrated nearby 90° (Fig. 19). Hence most of the synthetic earthquakes correspond to normal faulting.

For the eastern edge of Adria along the Dinarides (fault 9) the histogram of the slip values obtained for synthetic earthquakes has the maximum between -70° and -50° , that corresponds to reverse faulting with the considerable strike-slip component. For the south-eastern edge of Adria (fault 10) the slip component increases, here the maximum is between -30 ° and -10 ° (Fig. 20).

The comparison of the mechanisms for synthetic and observed seismicity sows the good agrrement.

6. Conclusion

The results of the numerical simulation of block structure dynamics for the Italian region show that it is possible to reproduce the main observed features of tectonic motions. Particularly, a counter-clockwise rotation of Adria is obtained. The extensional zone along the Apennines and the compressional zone along the north-western boundary of the Adriatic Sea are correctly reproduced.

The synthetic seismicity obtained in the model exhibits a quite good agreement with observed seismicity. The largest synthetic events are obtained in the Calabrian arc, in the Southern Apennines, south of the Ortona-Roccamonfina discontinuity, and in the Northern Dinarides near the conjunction with Eastern Alps. The rate of seismic activity in the Apennines increases from north to south; while the level of synthetic seismic activity is not high enough in the Southern Dinarides. The slope of the FM plot for synthetic seismicity is larger than for observed one; it can be a consequence of a lack of strong events in the Southern Dinarides.

The analysis of the source mechanisms of the synthetic earthquakes displays a quite good agreement with the available observations. Normal faulting is typical for synthetic seismicity obtained in the Apennines, the eastern edge of Sicily and the Calabrian arc, while in the north-western boundary of the Adriatic Sea, in the Southern Alps and along the eastern edge of Adria along the Dinarides reverse faulting predominates.

The results of the modeling give us possibility to conclude that the available observations can not be explained only as a consequence of the convergence of Africa and Europe. The processes controlling the tectonics and seismicity in the region are more complicated. It is possible, that the northern part of Adria is connected with Africa by the mantle flow, which extends to the Alps. At the same time there are some additional processes, which cause the presence of extensional – compressional belt in the Northern Apennines and the high level of seismicity in the Calabrian Arc. Taking into account the different coupling of blocks with the underlying medium as well as different features of the faults is also essential to recover the main characteristics of the observed seismicity.

We do not consider that we have proposed a perfectly adequate model of the block structure dynamics of Italian region. The model may be improved with the contribution of new kinematics observations and knowledge about the lithosphere structure of the Central Mediterranean area.

References

Aifa,T., H.Feinberg, and J.P.Pozzi (1988). Pliocene-Pleistocene evolution of the Tyrrhenian arc: paleomagnetic determination of uplift and rotational deformation. *Earth and Planet. Sci. Lett.*, **87**, 438-452.

Alekseevskaya,M.A., A.M.Gabrielov, A.D.Gvishiani, I.M.Gelfand, and E.Ya.Ranzman (1977). Formal morphostructural zoning of mountain territories. *J. Geophys.*, **43**, 227-233.

Anderson,H., and J.Jackson (1987). Active tectonics in the Adriatic region. *Geophys. J. R. Astr. Soc.*, **91**, 937-983.

Anzidei,M., P.Baldi, G.Casula, M.Crespi, and F.Riguzzi (1996). Repeated GPS surveys across the Ionian Sea: evidence of crustal deformations. *Geophys. J. Int.*, **127**, 257-267.

Calcagnile,G., and G.F.Panza (1981). The main characteristics of the litosphere-astenosphere system in Italy and surrounding regions. *Pure and Appl. Geophys.*, **119**, 865-879.

Caputo,M., G.F.Panza, and D.Postpischl (1970). Deep structure of the Mediterranean basin, *JGREA*, **75**, 4919.

Caputo,M., G.F.Panza, and D.Postpischl (1972). New evidence about the deep structure of the Lipari arc. *Tectonophysics*, **15**, 219.

Caputo,M., V.Keilis-Borok, E.Oficerova, E.Ranzman, I.Rotwain, and A.Solovieff (1980). Pattern recognition of earthquake-prone areas in Italy. *Phys. Earth Planet. Inter.*, **21**, 305-320.

Cisternas,A., P.Godefroy, A.Gvishiani, A.I.Gorshkov, V.Kosobokov, M.Lambert, E.Ranzman, J.Sallantin, H.Saldano, A.Soloviev, and C.Weber (1985). A dual approach to recognition of earthquake prone areas in the western Alps. Annales Geophysicae, **3**, 2, 249-270.

Della Vedova,B., I.Marson, G.F.Panza, and P.Suhadolc (1991). Upper mantle properties of the Tuscan-Tyrrhenian Area: a key for understanding the recent tectonic evolution of the italian region. *Tectonophys*, **195**, 311-318.

Gabrielov,A.M., T.A.Levshina, and I.M.Rotwain (1990). Block model of earthquake sequence. *Phys. Earth Planet. Inter.*, **61**, 18-28.

Geiger,A., H-G.Kahle, and E.Gubler (1986). Recent crustal movements in the Alpine-Mediterranean region analyzed in the Swiss Alps. *Tectonophysics*, **130**, 289-298.

Gorshkov,A.I., G.F.Panza, A.A.Soloviev, and A.Aoudia (2002). Morphostructural zonation and preliminary recognition of seismogenic nodes around the Adria margin in peninsular Italy and Sicily. *Journal of Seismology and Earthquake Engineering*, **3**, 2, 1-24.

Gripp,A.E. and Gordon,R.G. (1990). Current plate velocities relative to the hotspots incorporating the NUVEL-1 global plate motion model. *Geophys. Res. Lett.*, **17**, 8, 1109-1112.

Gubler,E., H-G.Kahle, and E.Klingele (1981). Recent crustal movements in Switzerland and their geophysical interpretation. *Tectonophysics*, **71**, 125-152.

Ismail-Zadeh, A.T., Keilis-Borok, V.I., and Soloviev, A.A. (1999) Numerical modelling of earthquake flow in the south-eastern Carpathians (Vrancea): effect of a sinking slab. *Phys. Earth Planet. Inter.*, **111**, 3-4, 267-274.

Keilis-Borok,V.I., I.M.Rotwain, and A.A.Soloviev (1997). Numerical modelling of block structure dynamics: dependence of a synthetic earthquake flow on the structure separateness and boundary movements. *J. Seismol.*, **1**, 151-160.

Leydecker,G. (1991). Historical Earthquake Catalogues: Central and southeastern Europe (342 BC - 1990). Web site: http://www.bgr.de/quakecat/eng/homepage.htm.

Maksimov,V.I., and A.A.Soloviev (1999). Clustering of earthquakes in a block model of lithosphere dynamics. In D.K.Chowdhury (ed.), *Computational Seismology and Geodynamics* / Am. Geophys. Un., **4**, Washington, D.C.: The Union, 124-126.

Marson,I., G.F.Panza, and P.Suhadolc (1995). Crust and upper mantle models along the active Tyrrhenian rim. *Terra Nova*, **7**, 348-357.

Meletti,C., E.Patacca, and P.Scandone (1995). Il sistema compressione-distensione in Appennino. In G.Bonardi, B.De Vivo, P.Gasperini, and A.Vallario (eds) *Cinquanta anni di attività didattica e scientifica del Prof. Felice Ippolito*. Liguori, Napoli, 361-370.

Meletti,C., E.Patacca, and P.Scandone (2000). Construction of a seismotectonic model: the case of Italy. *Pure Appl. Geophys.*, **157**, 11-35.

Panza,G.F. (1984). Structure of the lithosphere-asthenosphere system in the Mediterranean region. *Annales Geophys.*, **2**, 137-138.

Panza, G.F., A.A.Soloviev, and I.A.Vorobieva (1997). Numerical modelling of block-structure dynamics: Application to the Vrancea region. *Pure Appl. Geophys.*, **149**, 313-336.

Peresan,A., G.F.Panza, and G.Costa (2000). CN algorithm and long lasting changes in reported magnitudes: the case of Italy. *Geophys. J. Int.*, **141**, 425-437.

Press,F., and C.Allen (1995). Patterns of seismic release in the southern California region. *J. Geophys. Res.*, **100**, 6421-6430.

Sagnotti,L. (1992). Paleomagnetic evidence for a Pleistocene counterclockwise rotation of the Sant'Arcangelo basin, Southern Italy. *Geophys. Res. Lett.*, **19** (2), 135-138.

Sagnotti,L., C.Facenna, and R.Funiciello (1994). Paleomagnetic evidence for no tectonic rotation of the Central Italy Tyrrhenian margin since upper Pliocene. *Geophys. Res. Lett.*, **21** (6), 481-484.

Saraò,A., G.F.Panza, and P.Suhadolc (1997). Waveforms and polarities for exdended and point source studies. In *Proceedings of the Messina University Forum on "Geodynamics of the Calabrian Arc"*. Taormina, Italy.

Scandone,P., E.Patacca, C.Meletti, M.Bellatalla, N.Perilli, and U.Santini (1990). Struttura geologica, evoluzione cinematica e schema sismotettonico della penisola italiana. *Atti del Convegno GNDT*, **1**, 119-135.

Scandone,P., E.Patacca, C.Meletti, M.Bellatalla, N.Perilli, and U.Santini (1994). Seismotectonic zoning of the italian peninsula: revised version. *Working file NOV94.*

Soloviev,A.A, I.A.Vorobieva, and G.F.Panza (1999). Modelling of block-structure dynamics: Parametric study for Vrancea. *Pure and Appl. Geophys.*, **156**, 3, 395-420.

Soloviev,A.A., I.A.Vorobieva, and G.F.Panza (2000). Modelling of block structure dynamics for the Vrancea region: Source mechanisms of the synthetic earthquakes. *Pure and Appl. Geophys.*, **157**, 1-2, 97-110.

Soloviev,A., and A.Ismail-Zadeh (2003). Models of Dynamics of Block-and-Fault Systems. In V.I.Keilis-Borok and A.A.Soloviev (eds), *Nonlinear Dynamics of the Lithosphere and Earthquake Prediction.* Springer-Verlag, Berlin-Heidelberg, 71-139.

Utsu,T., and A.Seki, (1954). A Relation between the Area of Aftershock Region and the Energy of Main Shock. *J. Seismol. Soc. Japan*, 7, 233-240.

Vorobieva,I.A., A.I.Gorshkov, and A.A.Soloviev (2000). Modelling of the block structure dynamics and seismicity for the Western Alps. In V.I.Keilis-Borok and G.M.Molchan (eds), *Problems of Dynamics and Seismicity of the Earth.* Moscow, GEOS, 154-169 (Comput. Seismol.; Iss. 31, in Russian).

Ward,S.N. (1994). Constraints on the seismotectonics of the Central Mediterranean from Very Long Baseline Interferometry. *Geophys. J. Int.*, **117**, 441-452.

TABLE 1 Experiment 1

Prescribed velocities of underlying medium and resulted displacements of blocks

#block	Prescribed velocities of underlying medium			Displacements of blocks		
	Vx	*Vy*	*ω*	*dX*	*dY*	Angle
I	0	0	0	-26.01	-2.93	1.34
II	0	0	0	-3.97	6.68	-0.39
III	0	0	0	-22.71	2.56	2.02
IV	0	0	0	-66.59	91.84	5.17
V	0	0	0	24.33	11.60	-0.08
VI	0	0	0	102.90	261.46	16.09
VII	0	0	0	-68.06	55.15	-2.48
VIII	0	0	0	-151.22	197.53	-0.89
IX	0	0	0	-60.36	50.70	-6.55
X	0	0	0	-190.28	175.40	-19.35
XI	0	0	0	80.57	59.50	9.12

Prescribed velocities of boundary blocks

#Boundary block	*Vx*	*Vy*	*ω*
BB1-BB3, BB6-BB9	0	0	0
BB4	-25.00	65.00	0
BB5	-25.00	65.00	0

TABLE 2 Experiment 2 (Depth 15 km)

Prescribed velocities of underlying medium and resulted displacements of blocks

#block	Prescribed velocities of underlying medium			Displacements of blocks		
	Vx	*Vy*	*ω*	*dX*	*dY*	Angle
I	0	0	0	-6.86	-0.17	0.28
II	0	0	0	-2.32	2.07	-0.17
III	0	0	0	-6.63	-0.81	0.59
IV	0	0	0	-27.33	36.98	2.19
V	0	0	0	7.70	0.85	0.22
VI	0	0	0	32.57	114.34	7.58
VII	0	0	0	-31.55	40.09	-1.93
VIII	0	0	0	-87.08	103.98	-1.21
IX	0	0	0	-27.68	28.84	-5.30
X	0	0	0	-140.00	106.26	-16.18
XI	0	0	0	30.19	24.97	4.39

Prescribed velocities of boundary blocks

#Boundary block	*Vx*	*Vy*	*ω*
BB1-BB3, BB6-BB9	0	0	0
BB4	-25.00	65.00	0
BB5	-25.00	65.00	0

TABLE 3 Experiment 3

Prescribed velocities of underlying medium and resulted displacements of blocks

#block	Prescribed velocities of underlying medium			Displacements of blocks		
	Vx	*Vy*	*ω*	*dX*	*dY*	Angle
I	0	0	0	-148.48	108.06	12.90
II	0	0	0	37.31	96.13	-1.54
III	0	0	0	4.68	119.94	1.90
IV	1.20	45.60	0	33.94	767.95	8.49
V	33.30	54.60	0	406.57	823.74	26.11
VI	33.50	77.30	0	673.85	1340.63	8.07
VII	062.70	65.000	0	783.82	317.88	-21.06
VIII	69.60	74.10	0	1286.22	1373.10	-0.94
IX	0	0	0	73.57	132.34	0.57
X	0	0	0	-355.93	1191.13	1.02
XI	44.40	63.70	0	720.75	1125.58	19.83

Prescribed velocities of boundary blocks

#Boundary block	*Vx*	*Vy*	*ω*
BB1-BB3, BB6-BB9	0	0	0
BB4	69.60	74.10	0
BB5	-25.00	65.00	0

TABLE 4 Experiment 4

Prescribed velocities of underlying medium and resulted displacements of blocks

#block	Prescribed velocities of underlying medium			Displacements of blocks		
	Vx	*Vy*	*ω*	*dX*	*dY*	Angle
I	0	0	0	-139.14	110.16	12.46
II	0	0	0	39.52	99.14	-1.58
III	55.00	45.00	0	461.27	652.64	-6.06
IV	1.20	45.60	0	107.54	834.56	7.10
V	33.30	54.60	0	491.55	837.78	19.54
VI	33.50	77.30	0	677.09	1342.99	7.09
VII	062.70	65.000	0	766.86	325.59	-22.89
VIII	69.60	74.10	0	1284.96	1373.72	-0.98
IX	0	0	0	-256.30	189.63	9.63
X	0	0	0	-365.48	1198.77	1.49
XI	44.40	63.70	0	741.79	1096.82	22.15

Prescribed velocities of boundary blocks

#Boundary block	*Vx*	*Vy*	*ω*
BB1-BB3, BB6, BB8-BB9	0	0	0
BB4	69.60	74.10	0
BB5	-25.00	65.00	0
BB7	-30.00	30.00	0

TABLE 5 Experiment 5

Prescribed velocities of underlying medium and resulted displacements of blocks

#block	Prescribed velocities of underlying medium			Displacements of blocks		
	Vx	*Vy*	*ω*	*dX*	*dY*	Angle
I	0	0	0	-129.80	100.92	11.58
II	0	0	0	33.70	89.27	-1.22
III	55.00	45.00	0	638.37	728.83	-11.13
IV	1.20	45.60	0	123.90	842.10	7.25
V	33.30	54.60	0	549.00	867.17	17.45
VI	33.50	77.30	0	680.59	1341.60	7.19
VII	62.70	65.000	0	920.18	399.97	-17.08
VIII	69.60	74.10	0	1295.89	1371.29	-0.86
IX	0	0	0	-255.99	189.50	9.66
X	0	0	0	-365.82	1199.15	1.49
XI	44.40	63.70	0	757.07	1095.01	21.82

Prescribed velocities of boundary blocks

#Boundary block	*Vx*	*Vy*	*ω*
BB1-BB3, BB6, BB8-BB9	0	0	0
BB4	69.60	74.10	0
BB5	-25.00	65.00	0
BB7	-30.00	30.00	0

TABLE 6 Experiment 6

Prescribed velocities of underlying medium and resulted displacements of blocks

#block	Prescribed velocities of underlying medium			Displacements of blocks		
	Vx	*Vy*	*ω*	*dX*	*dY*	Angle
I	0	0	0	-141.84	110.46	11.85
II	0	0	0	13.07	125.18	-0.56
III	55.00	45.00	0	929.60	904.87	-15.68
IV	1.20	45.60	0	133.55	878.23	6.54
V	33.30	54.60	0	708.52	1031.95	8.34
VI	33.50	77.30	0	723.40	1395.68	6.11
VII	62.70	65.00	0	1216.02	493.51	-1.59
VIII	69.60	74.10	0	1373.14	1416.92	-0.06
IX	0	0	0	1.10	62.15	1.25
X	0	0	0	-436.41	1266.30	0.53
XI	44.40	63.70	0	822.69	1171.53	20.44

Prescribed velocities of boundary blocks

#Boundary block	*Vx*	*Vy*	*ω*
BB1-BB3, BB6, BB8-BB9	0	0	0
BB4	69.60	74.10	0
BB5	-25.00	65.00	0
BB7	-30.00	30.00	0

FIGURE CAPTIONS

Figure 1. Definitions used in the block-structure model.

Figure 2. Geodynamic model of Italy. Structural sketch (Meletti et al., 2000)

Figure 3. Geometry of the block structure. I – XI – blocks of structure, BB1- BB9 – boundary blocks

Figure 4. Observed seismicity.

Figure 5. Synthetic seismicity: Experiment 1

Figure 6. Synthetic seismicity: Experiment 2.

Figure 7. Synthetic seismicity: Experiment 3.

Figure 8. Synthetic seismicity: Experiment 4.

Figure 9. Synthetic seismicity: Experiment 5.

Figure 10. Synthetic seismicity: Experiment 6.

Figure 11. Movements (arrows) and rotations (curved arrows) obtained for the eleven blocks considered for the numerical simulation (experiment 6). Exact values of the resulting movements are given in Table 6.

Figure 12. Frequency-magnitude distribution for the synthetic (full circles) and observed (open circles) seismicity

Figure 13. Fault plane solutions for Italian region (Saraò et al., 1997).

Figure 14. Distribution of the slip angles for the synthetic earthquakes along the Northern Apennines (faults 28, 29).

Figure 15. Distribution of the slip angles for the synthetic earthquakes along the Southern Apennines (faults 30, 32).

Figure 16. Distribution of the slip angles for the synthetic earthquakes, along the compressional belt in Northern Apennines (faults 25, 26 and 27).

Figure 17. Distribution of the slip angles for the Southern Alps (fault 24).

Figure 18. Distribution of the slip angles for the synthetic earthquakes in the Calabrian Arc (faults 19 and 20).

Figure 19 Distribution of the slip angles for the synthetic earthquakes in the eastern edge of Sicily (fault 15).

Figure 20 Distribution of the slip angles for the synthetic earthquakes in the eastern edge of Adria (faults 9 and 10).

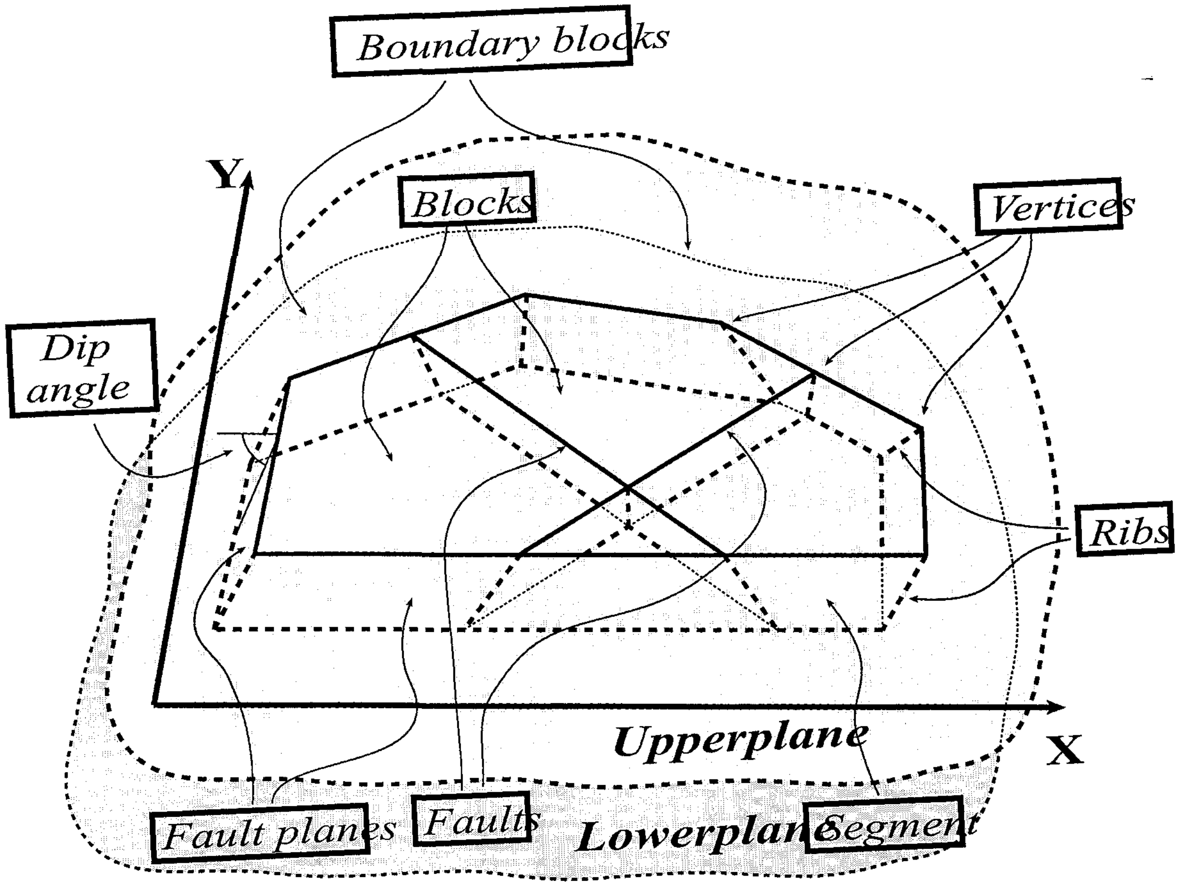

Boundary blocks
Y
Blocks
Vertices
Dip angle
Ribs
Upperplane
X
Fault planes
Faults
Lowerplane
Segment

Figure 1

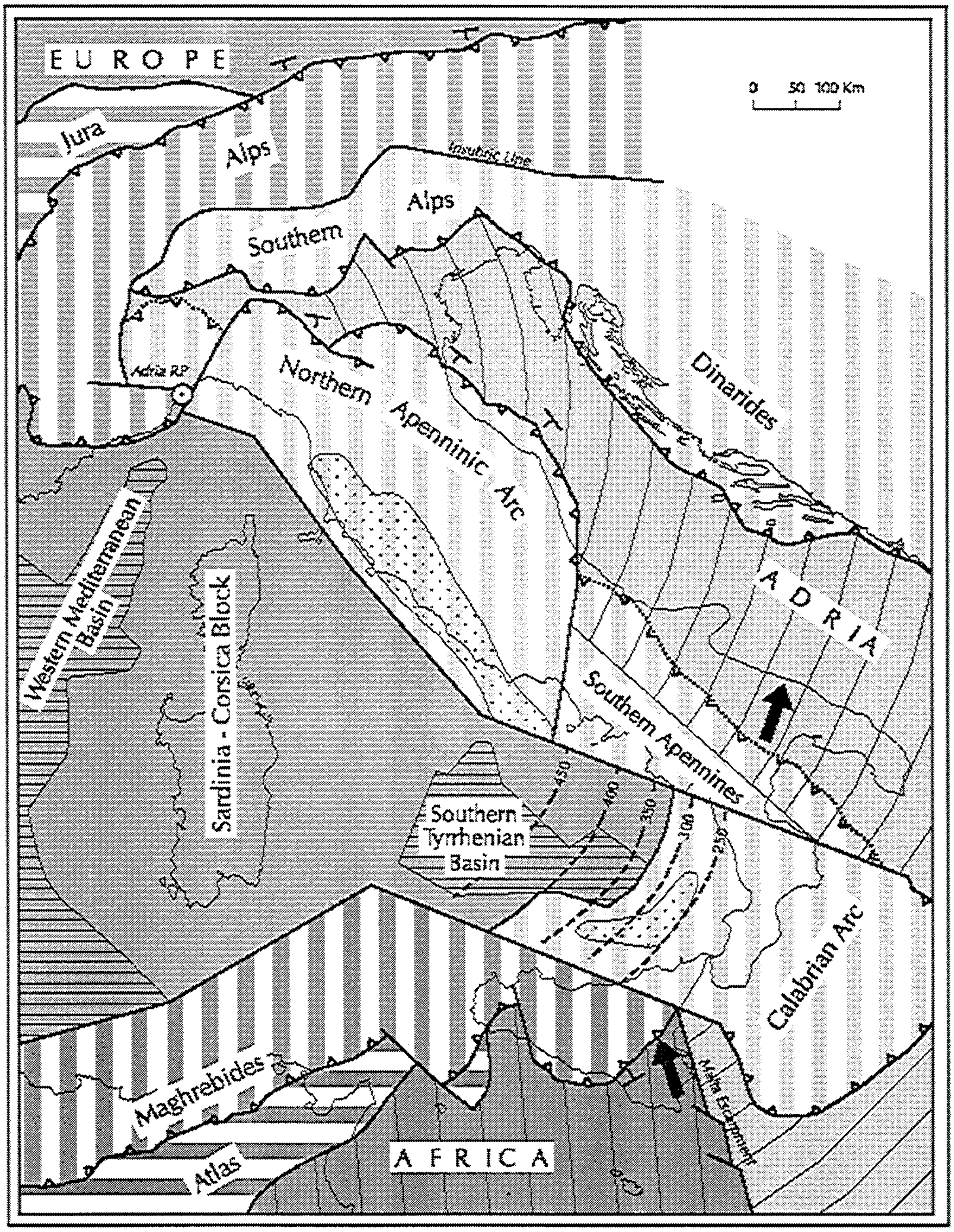
EUROPE
0 50 100 Km
Jura
Alps
Insubric Line
Southern
Alps
Adria RP
Northern Apenninic Arc
Dinarides
Western Mediterranean Basin
Sardinia - Corsica Block
ADRIA
Southern Apennines
450
400
350
300
250
Southern Tyrrhenian Basin
Calabrian Arc
Maghrebides
Atlas
AFRICA
Malta Escarpment

Figure 2

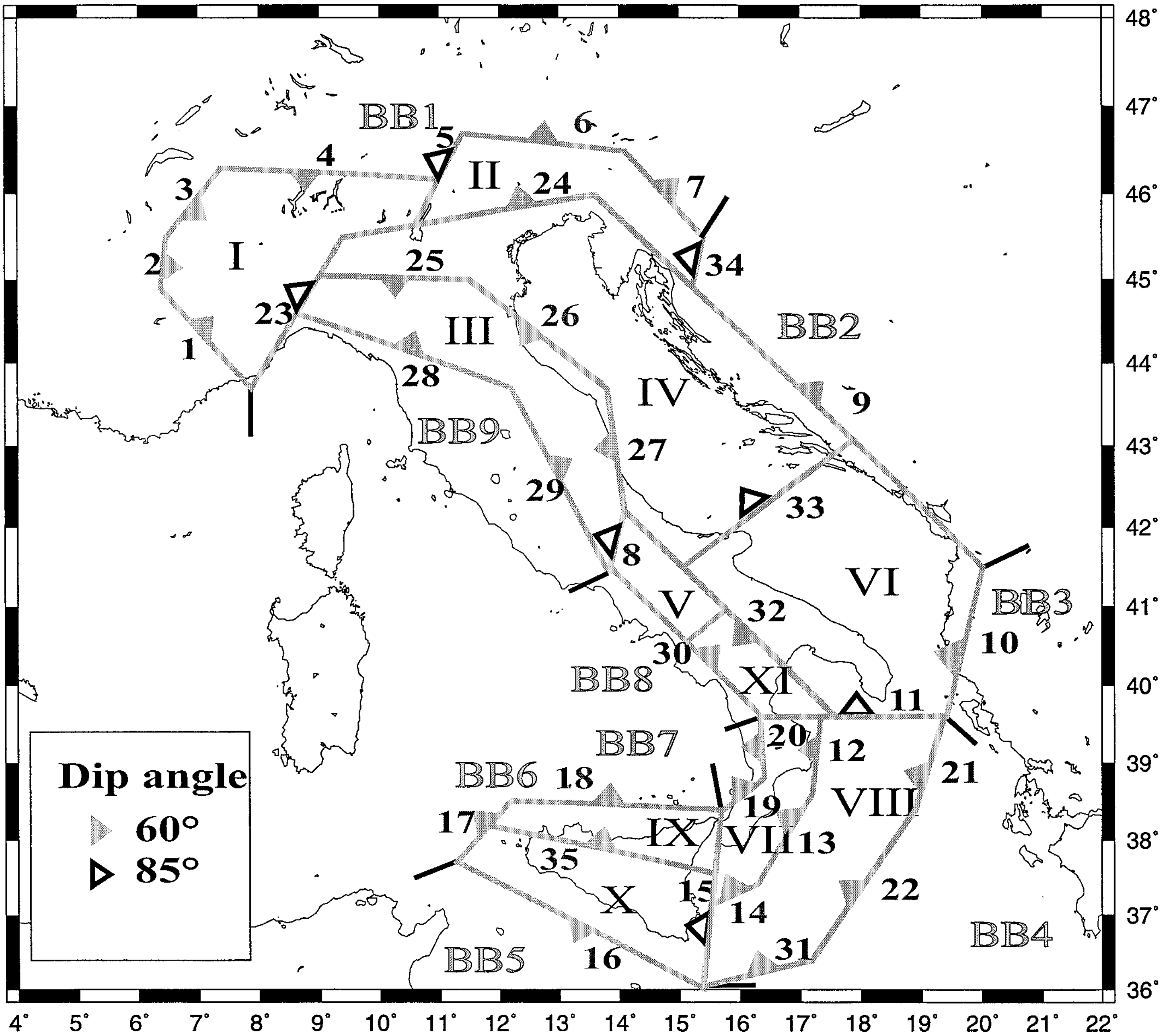
Dip angle
60°
85°
BB1
BB2
BB3
BB4
BB5
BB6
BB7
BB8
BB9
I
II
III
IV
V
VI
VII
VIII
IX
X
XI
48°
47°
46°
45°
44°
43°
42°
41°
40°
39°
38°
37°
36°
4°
5°
6°
7°
8°
9°
10°
11°
12°
13°
14°
15°
16°
17°
18°
19°
20°
21°
22°

Figure 3

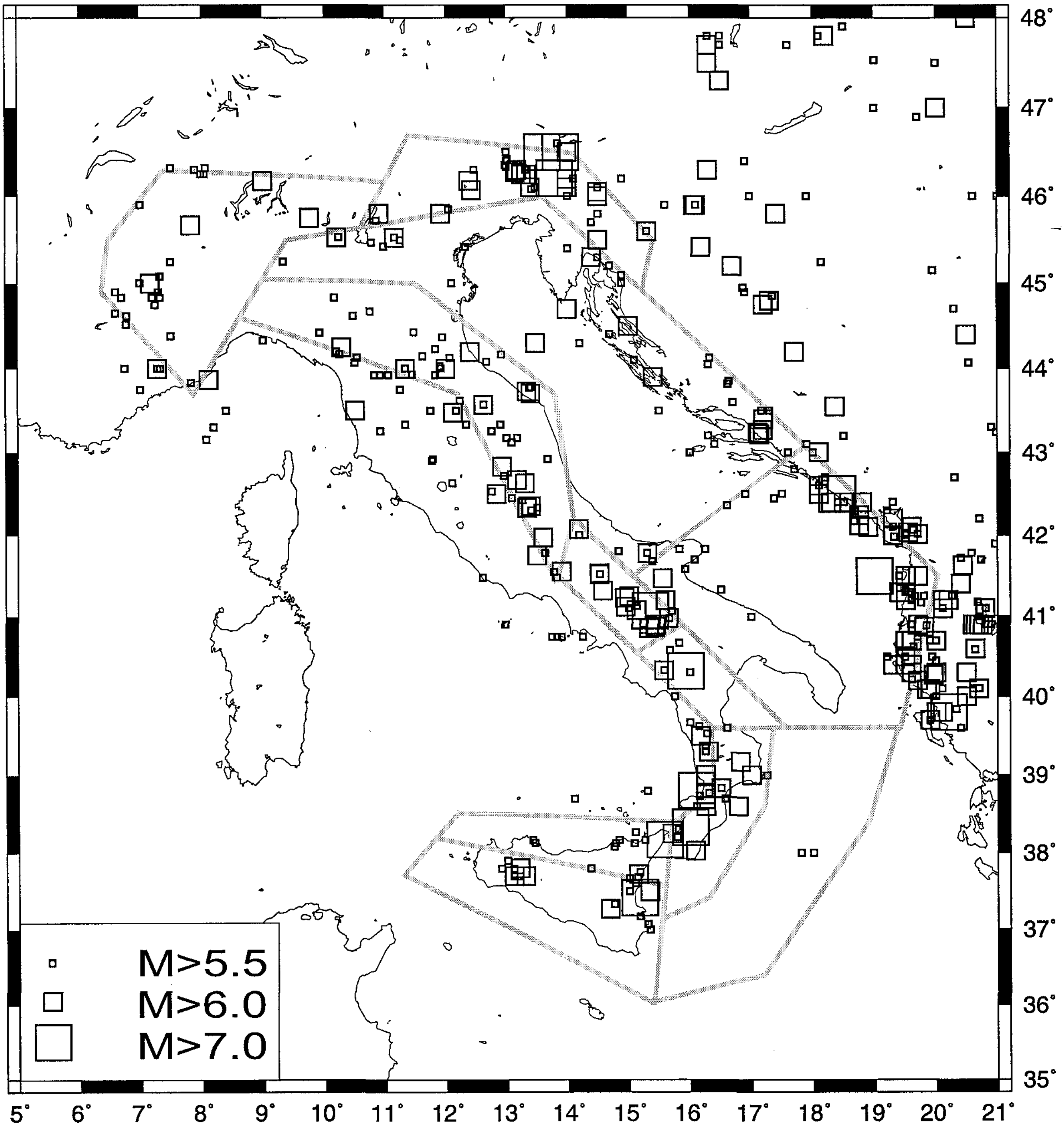
M>5.5
M>6.0
M>7.0
48°
47°
46°
45°
44°
43°
42°
41°
40°
39°
38°
37°
36°
35°
5°
6°
7°
8°
9°
10°
11°
12°
13°
14°
15°
16°
17°
18°
19°
20°
21°

Figure 4

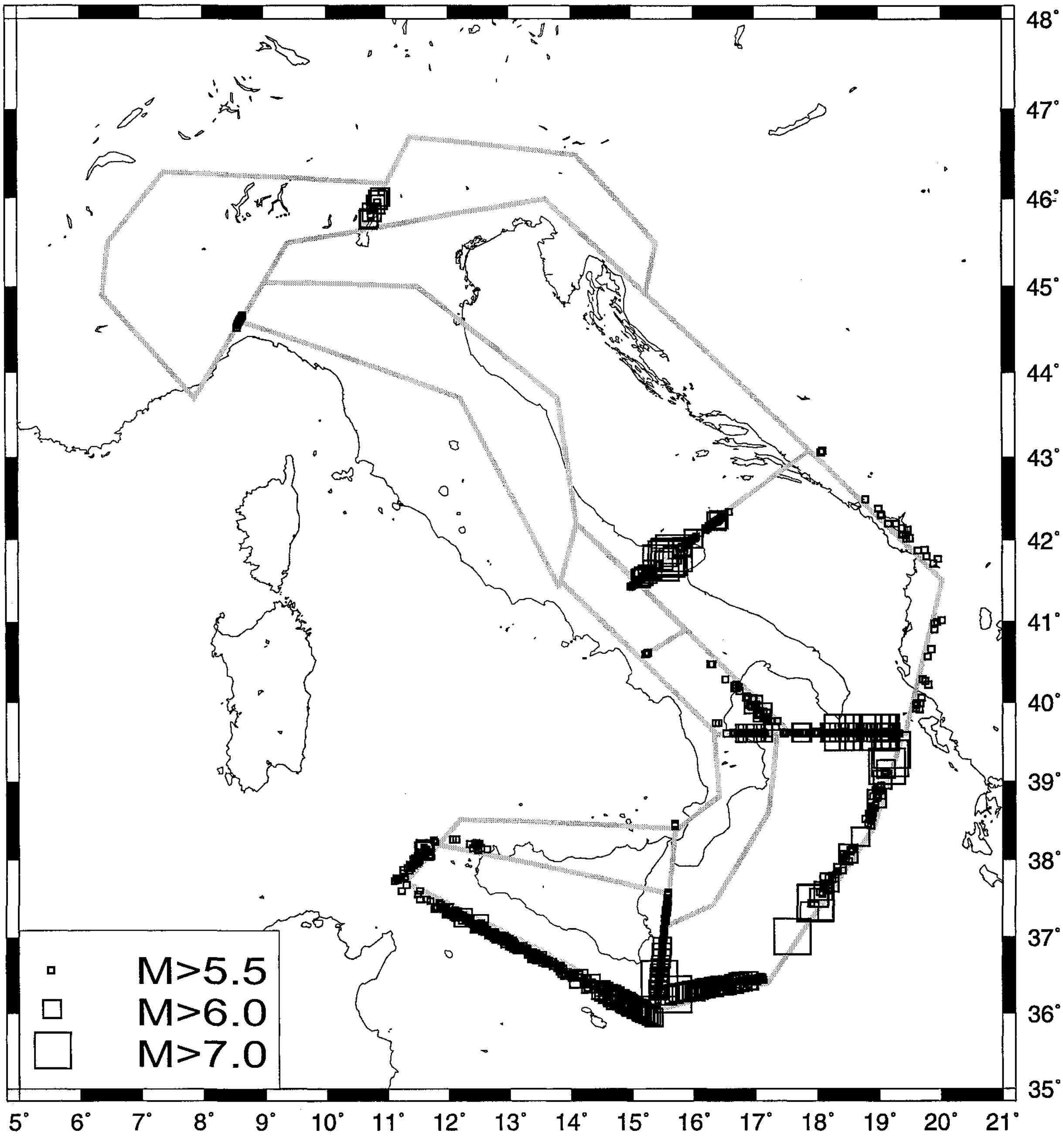

Synthetic seismicity: experiment 1

Figure 5

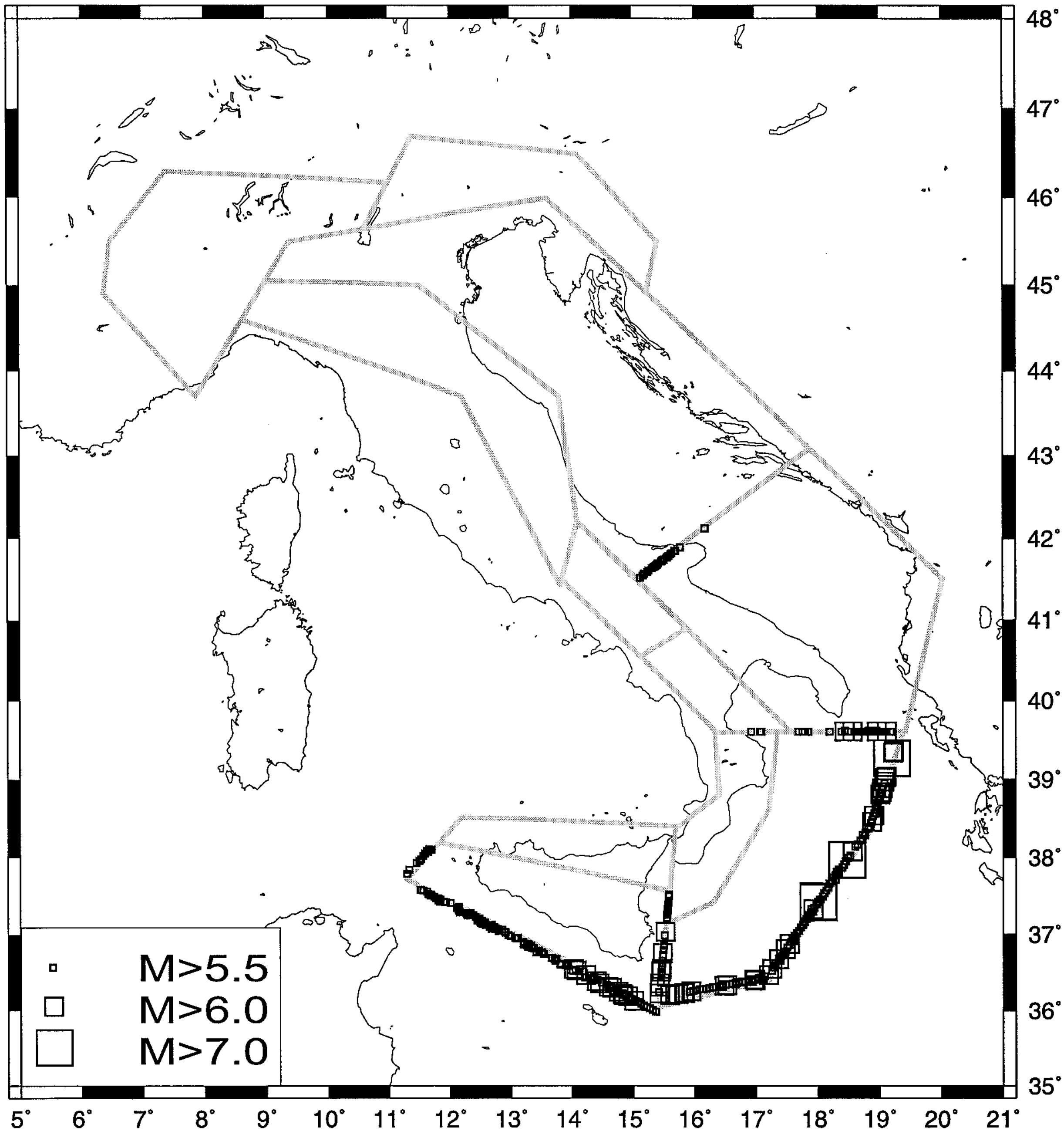

Synthetic seismicity: experiment 2

Figure 6

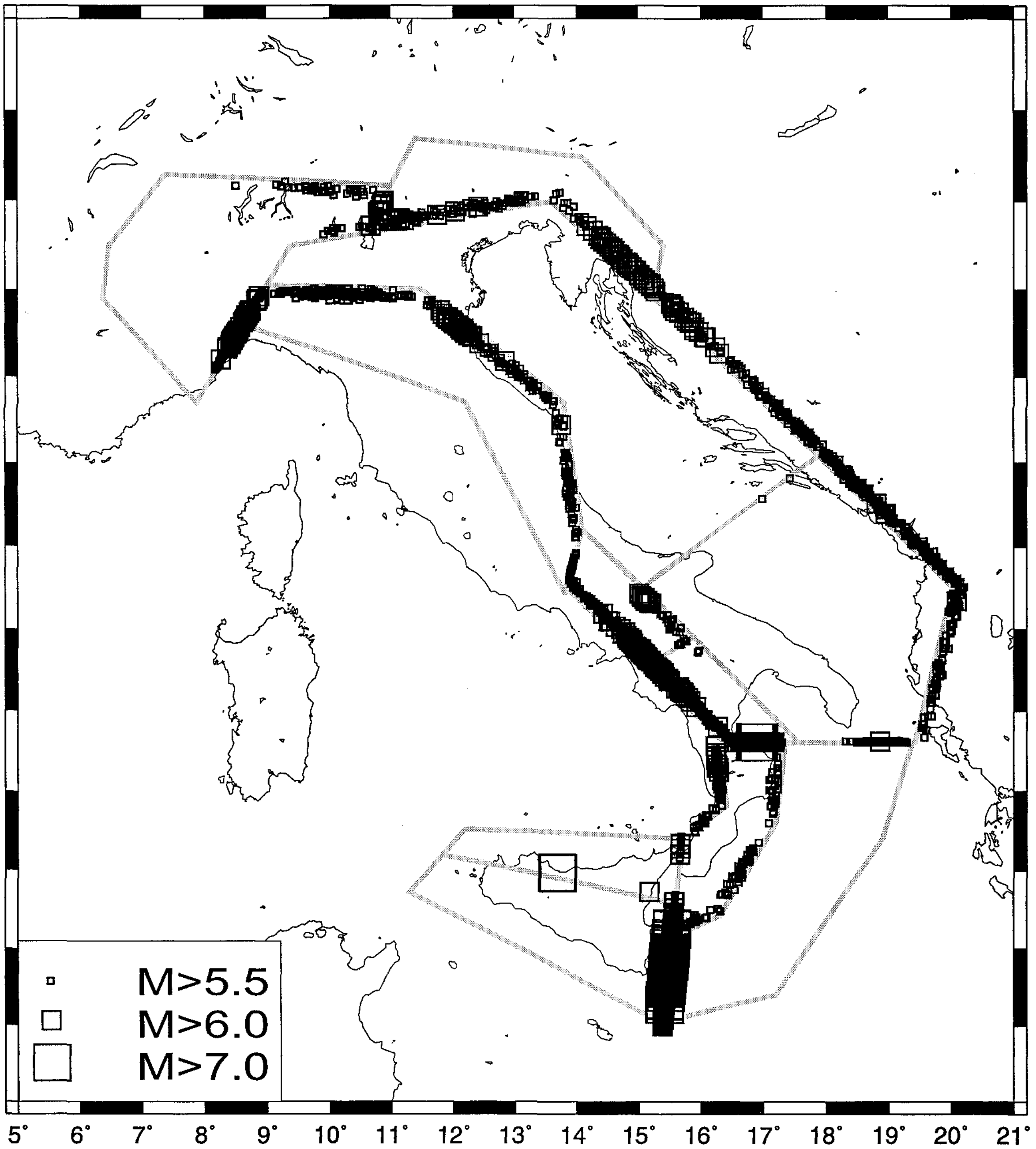

Synthetic seismicity: experiment 3

Figure 7

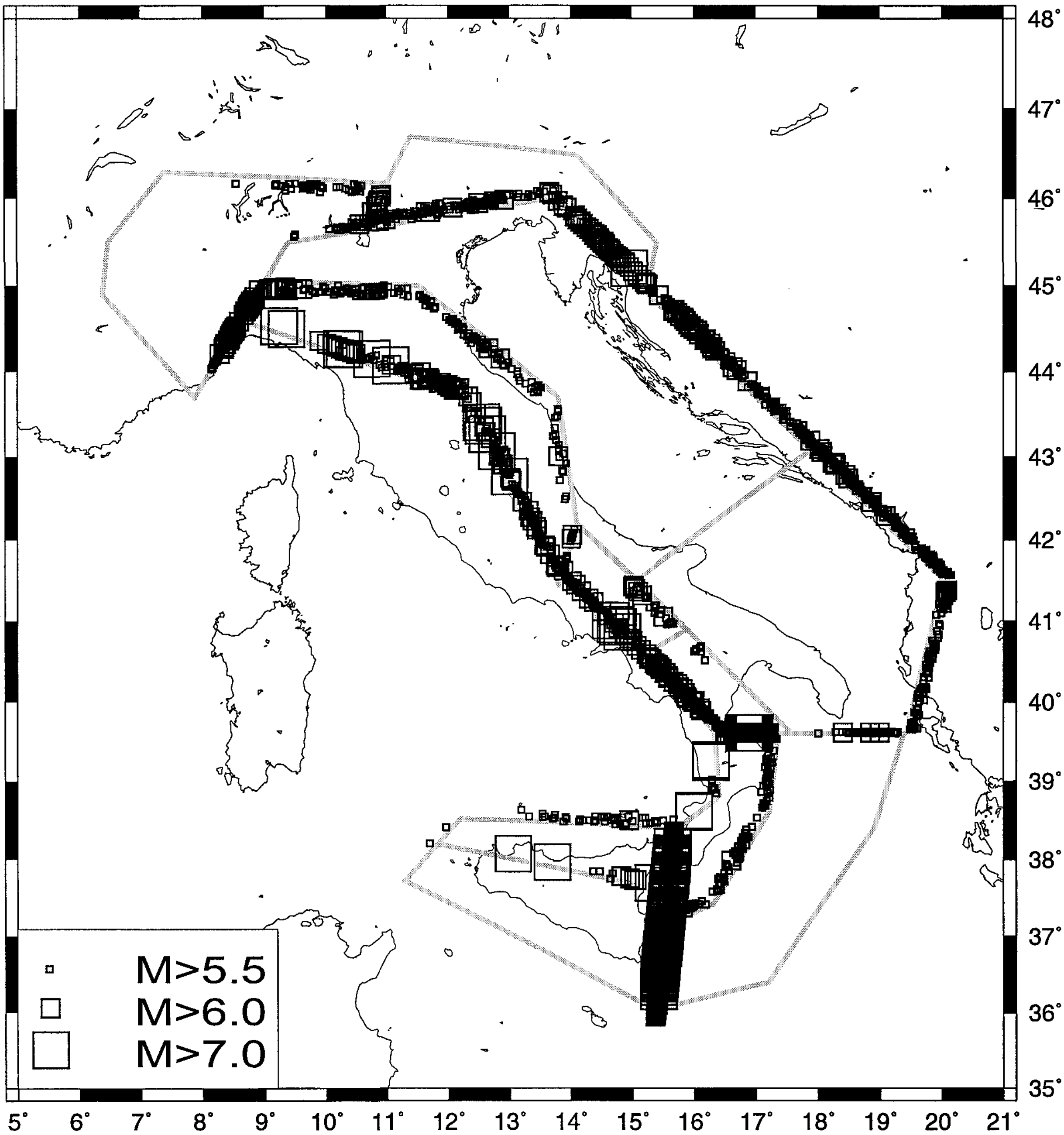

Synthetic seismicity: experiment 4

Figure 8

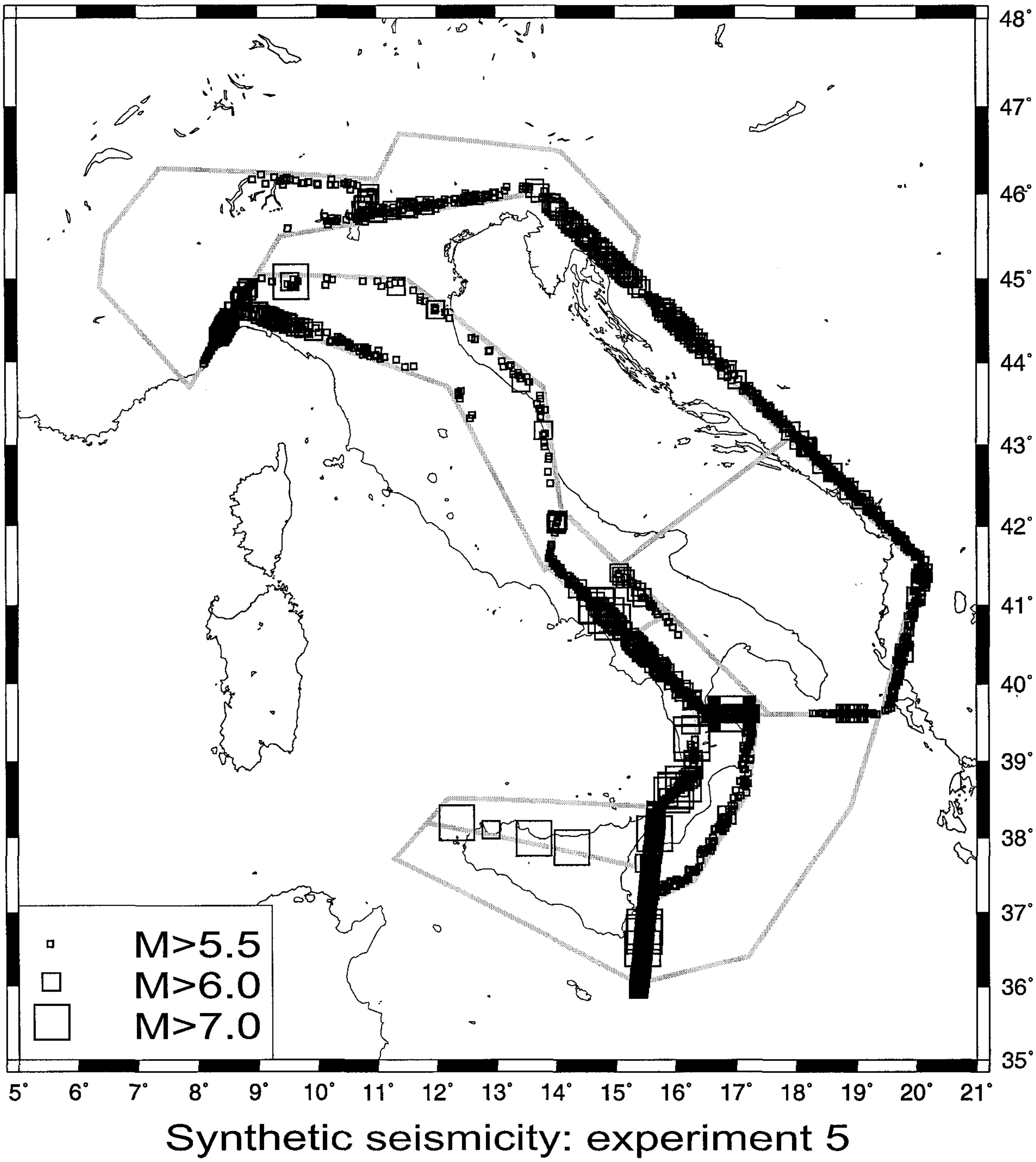

48°
47°
46°
45°
44°
43°
42°
41°
40°
39°
38°
37°
36°
35°
5°
6°
7°
8°
9°
10°
11°
12°
13°
14°
15°
16°
17°
18°
19°
20°
21°
M>5.5
M>6.0
M>7.0
Synthetic seismicity: experiment 5

Figure 9

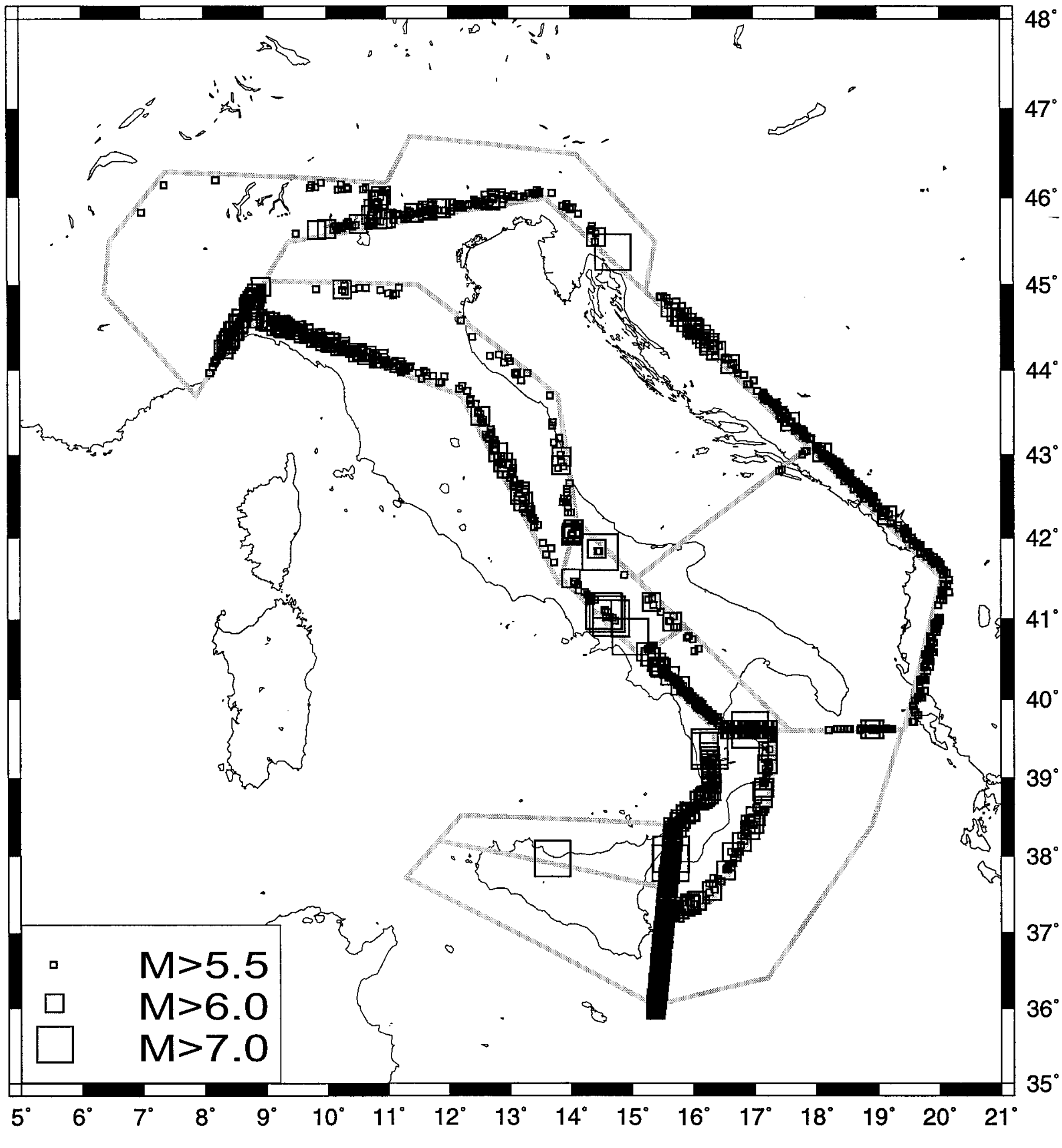

Synthetic seismicity: experiment 6
pole of rotation 44.2N 8.3E (Meletti 2000)

Figure 10

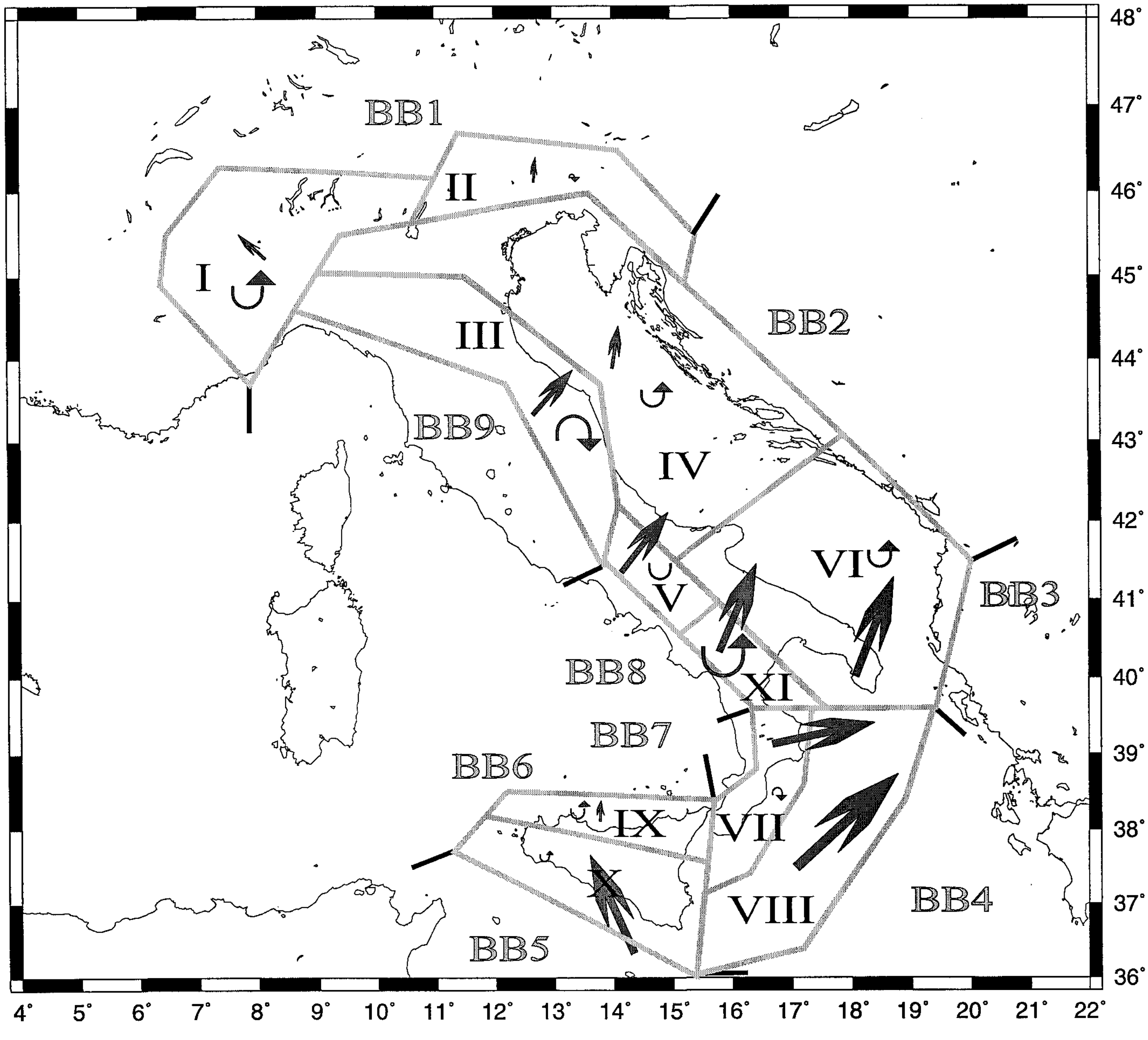

BB1
II
I
III
IV
BB2
BB9
VI
V
BB3
BB8
XI
BB7
BB6
IX
VII
X
VIII
BB4
BB5
48°
47°
46°
45°
44°
43°
42°
41°
40°
39°
38°
37°
36°
4°
5°
6°
7°
8°
9°
10°
11°
12°
13°
14°
15°
16°
17°
18°
19°
20°
21°
22°

Figure 11

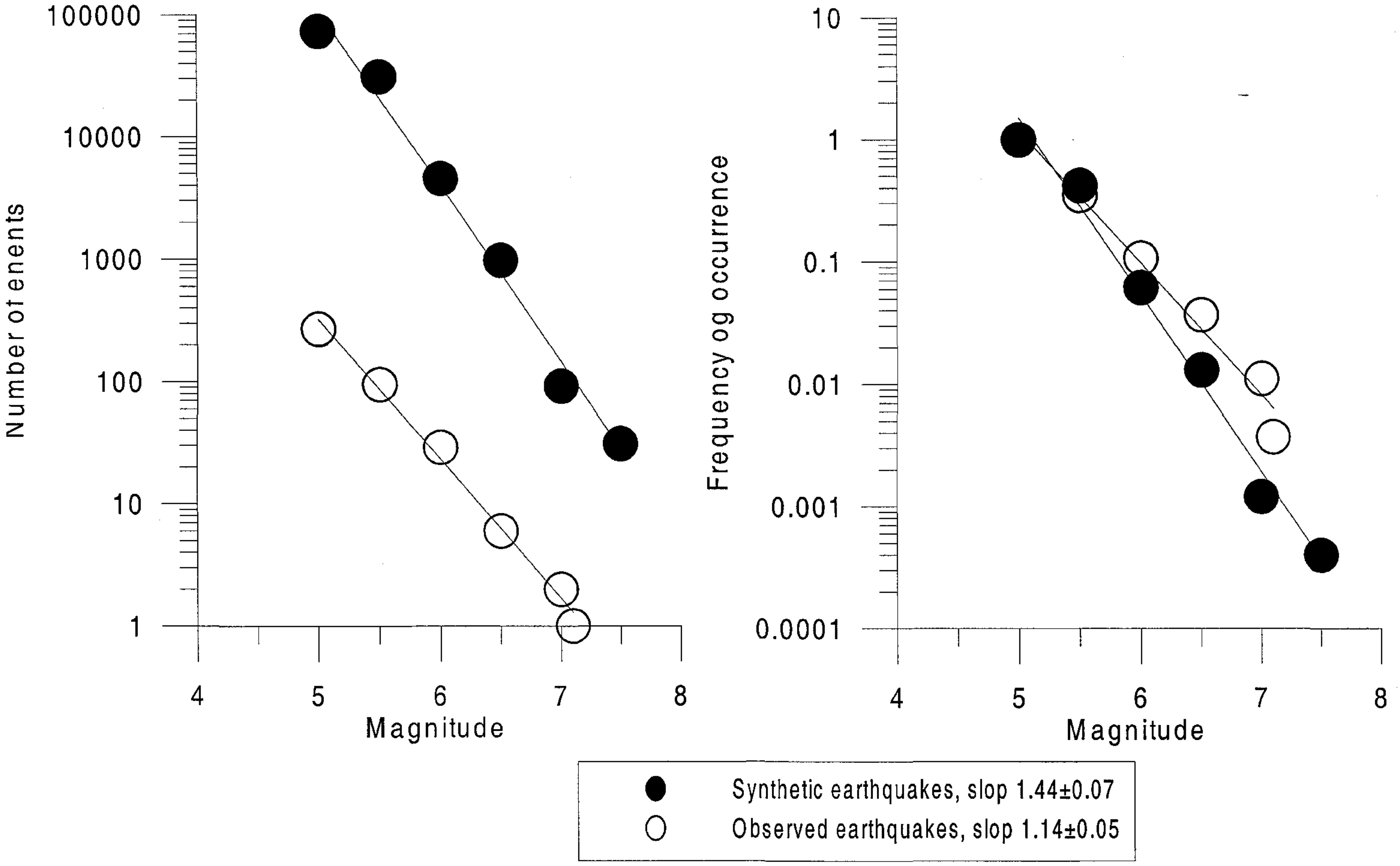

100000
10000
1000
100
10
1
Number of enents
4
5
6
7
8
Magnitude
10
1
0.1
0.01
0.001
0.0001
Frequency og occurrence
4
5
6
7
8
Magnitude
Synthetic earthquakes, slop 1.44±0.07
Observed earthquakes, slop 1.14±0.05

Figure 12

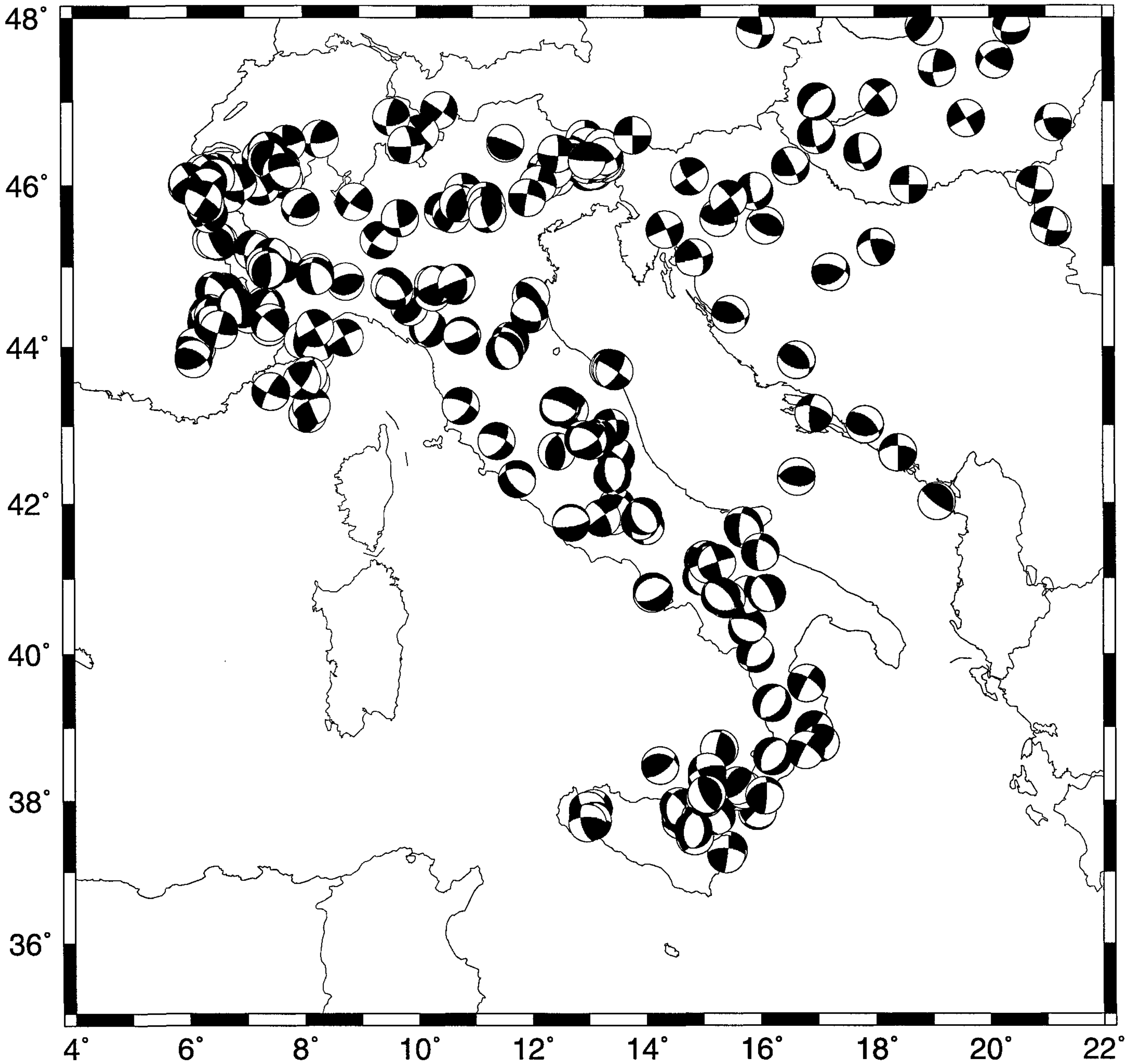

Figure 13

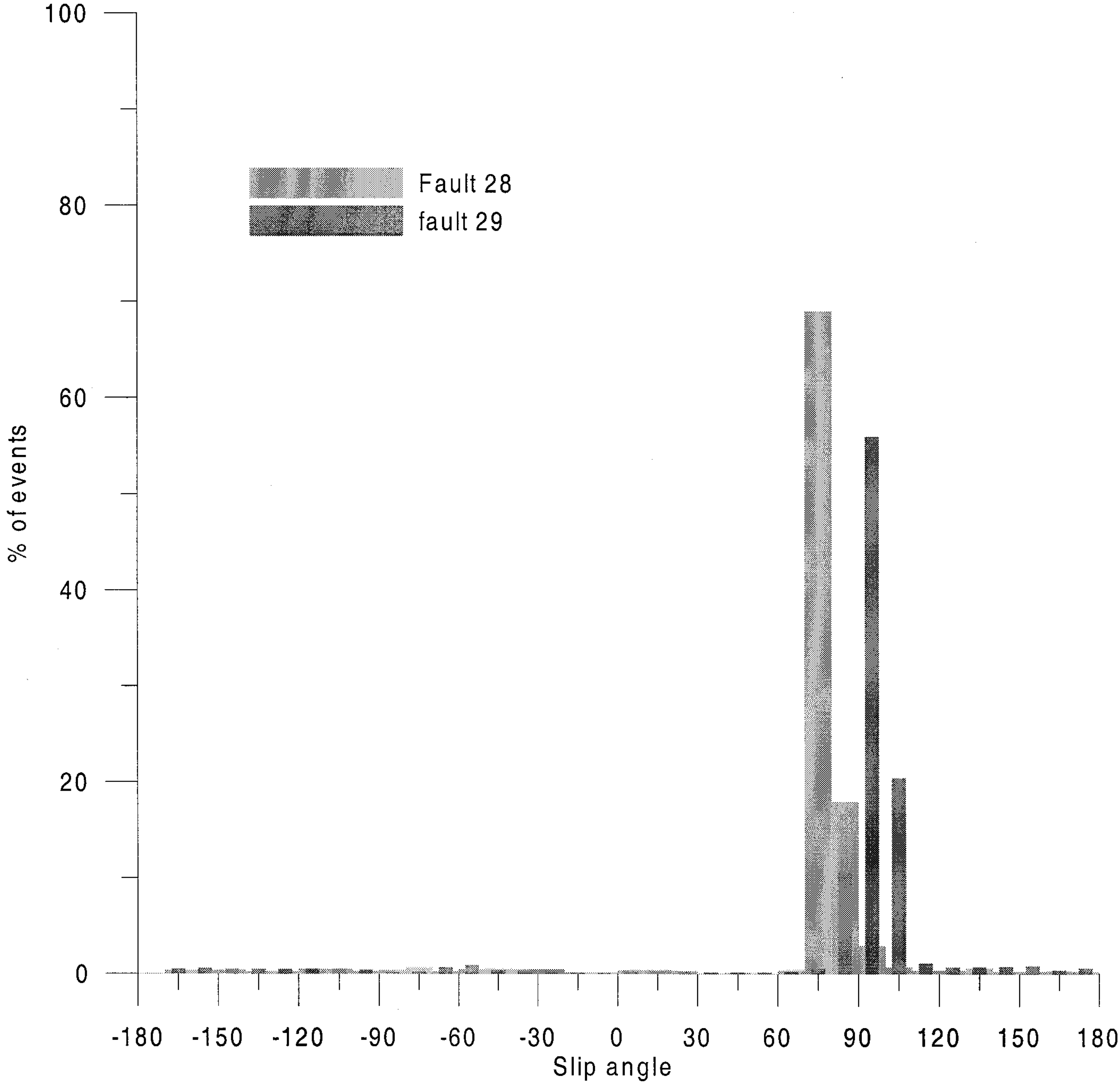
Fault 28
fault 29
100
80
60
40
20
0
% of events
-180
-150
-120
-90
-60
-30
0
30
60
90
120
150
180
Slip angle

Figure 14

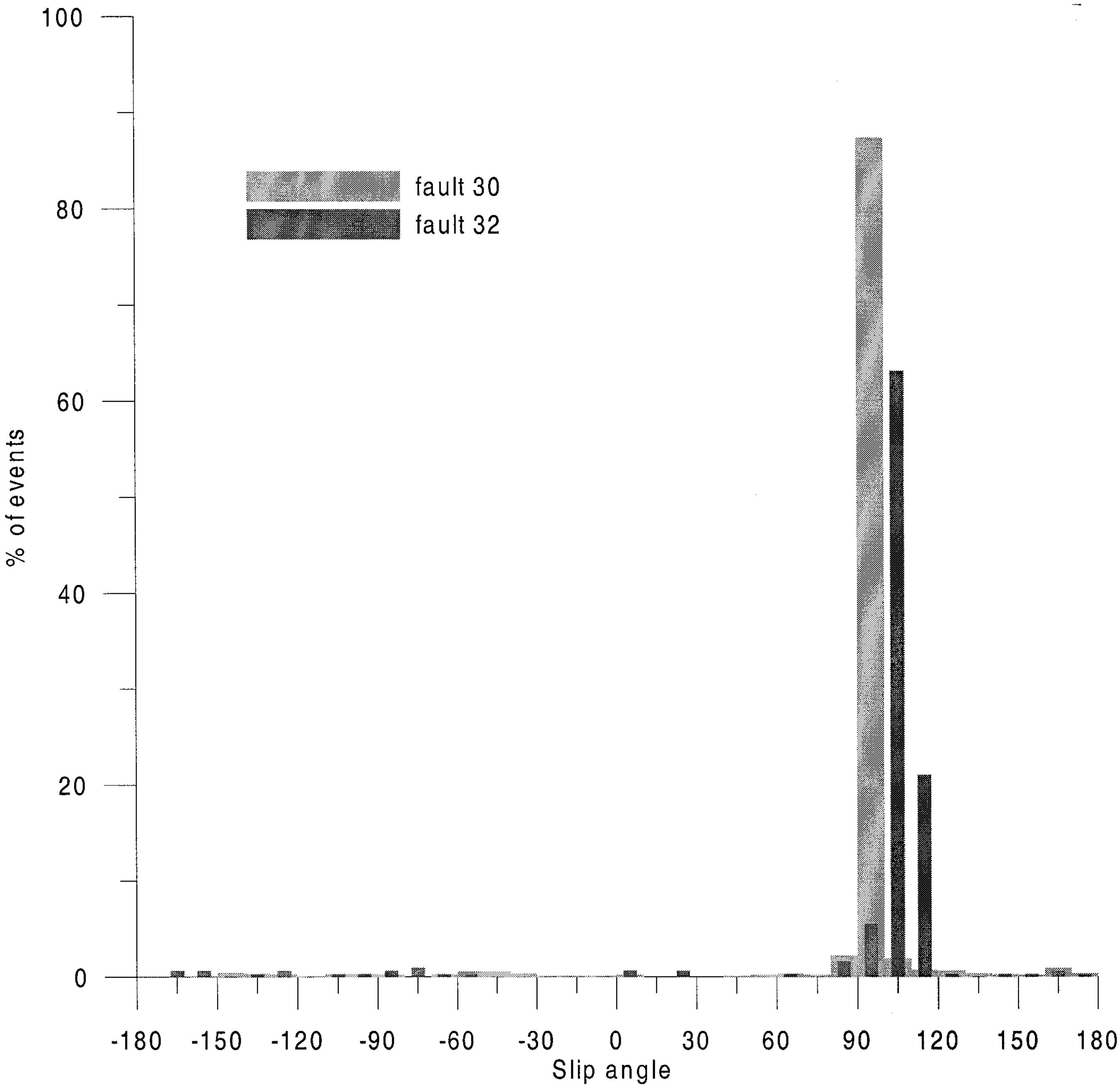
100
80
60
40
20
0
% of events
fault 30
fault 32
-180
-150
-120
-90
-60
-30
0
30
60
90
120
150
180
Slip angle

Figure 15

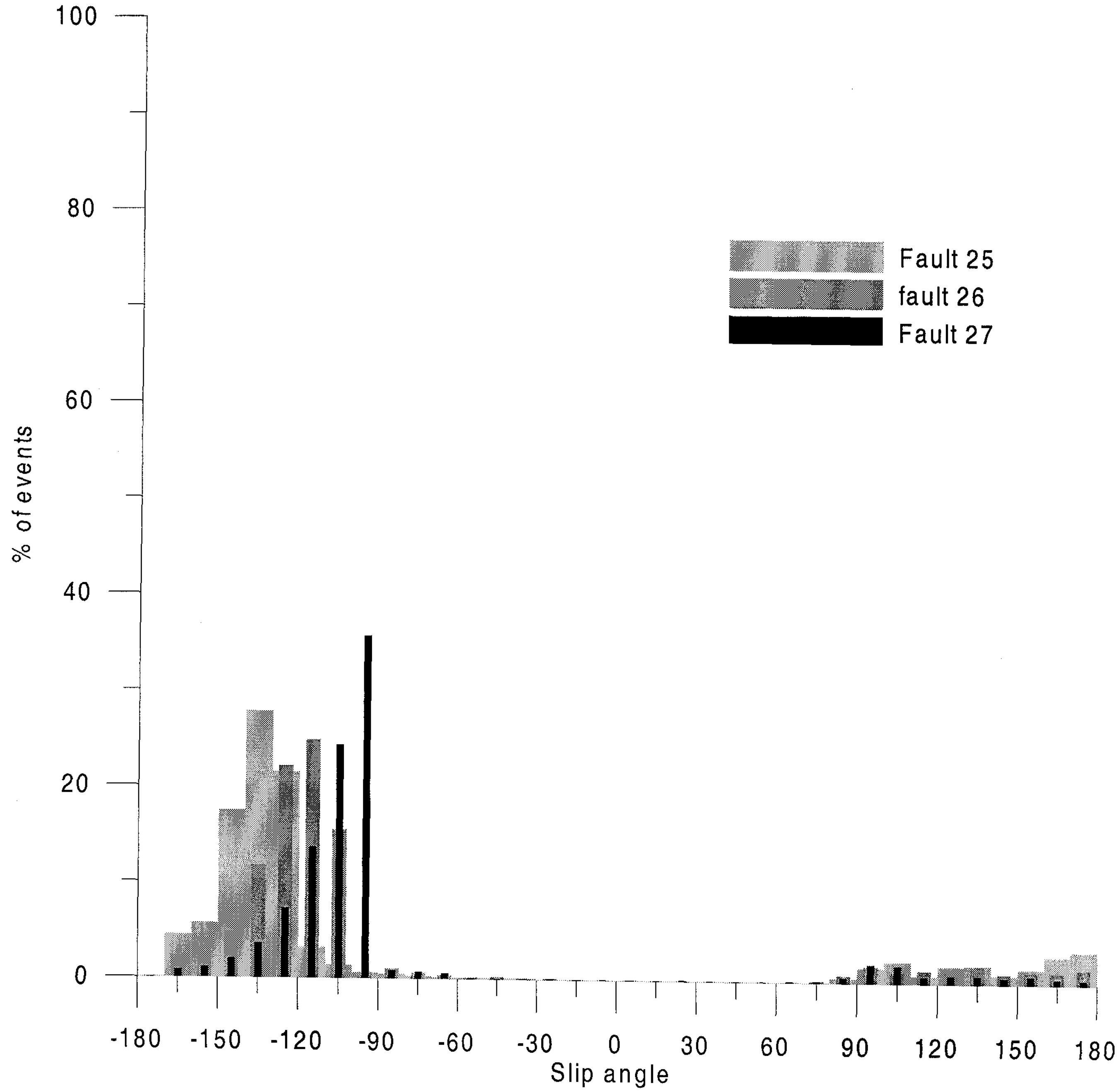

100
80
60
40
20
0
% of events
Fault 25
fault 26
Fault 27
-180
-150
-120
-90
-60
-30
0
30
60
90
120
150
180
Slip angle

Figure 16

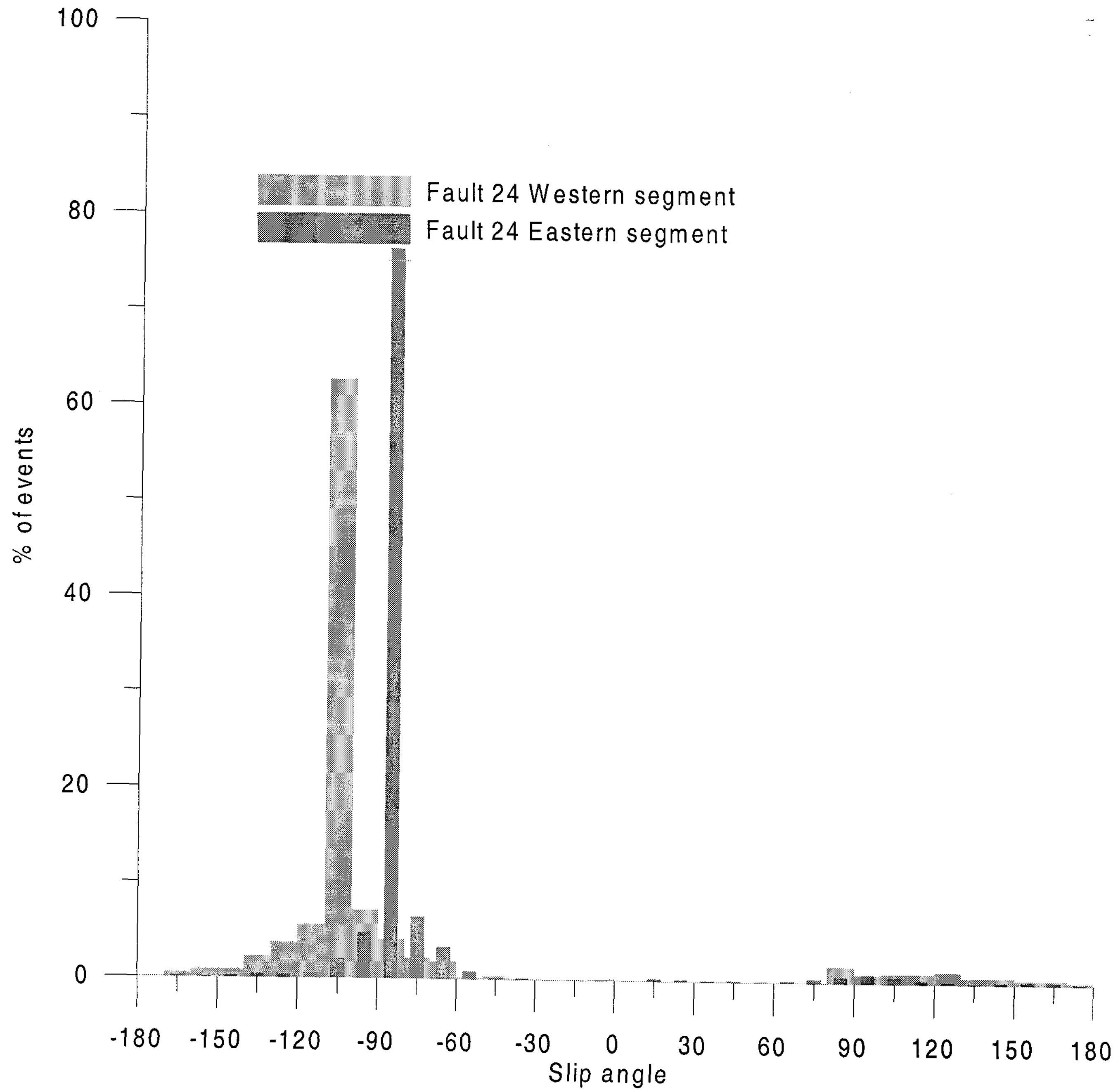
Fault 24 Western segment
Fault 24 Eastern segment
% of events
100
80
60
40
20
0
-180
-150
-120
-90
-60
-30
0
30
60
90
120
150
180
Slip angle

Figure 17

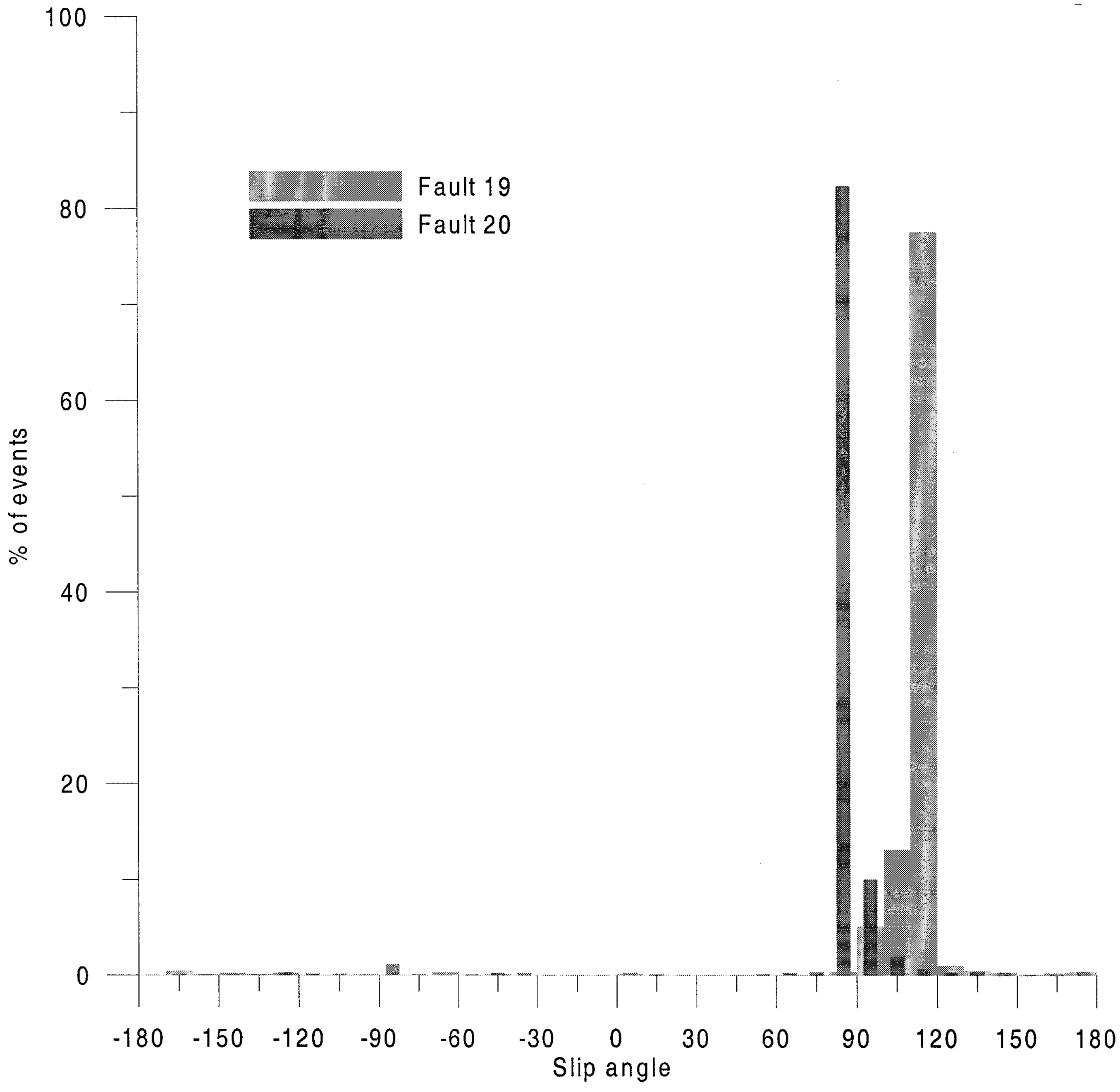

100
80
60
40
20
0
% of events
Fault 19
Fault 20
-180
-150
-120
-90
-60
-30
0
30
60
90
120
150
180
Slip angle

Figure 18

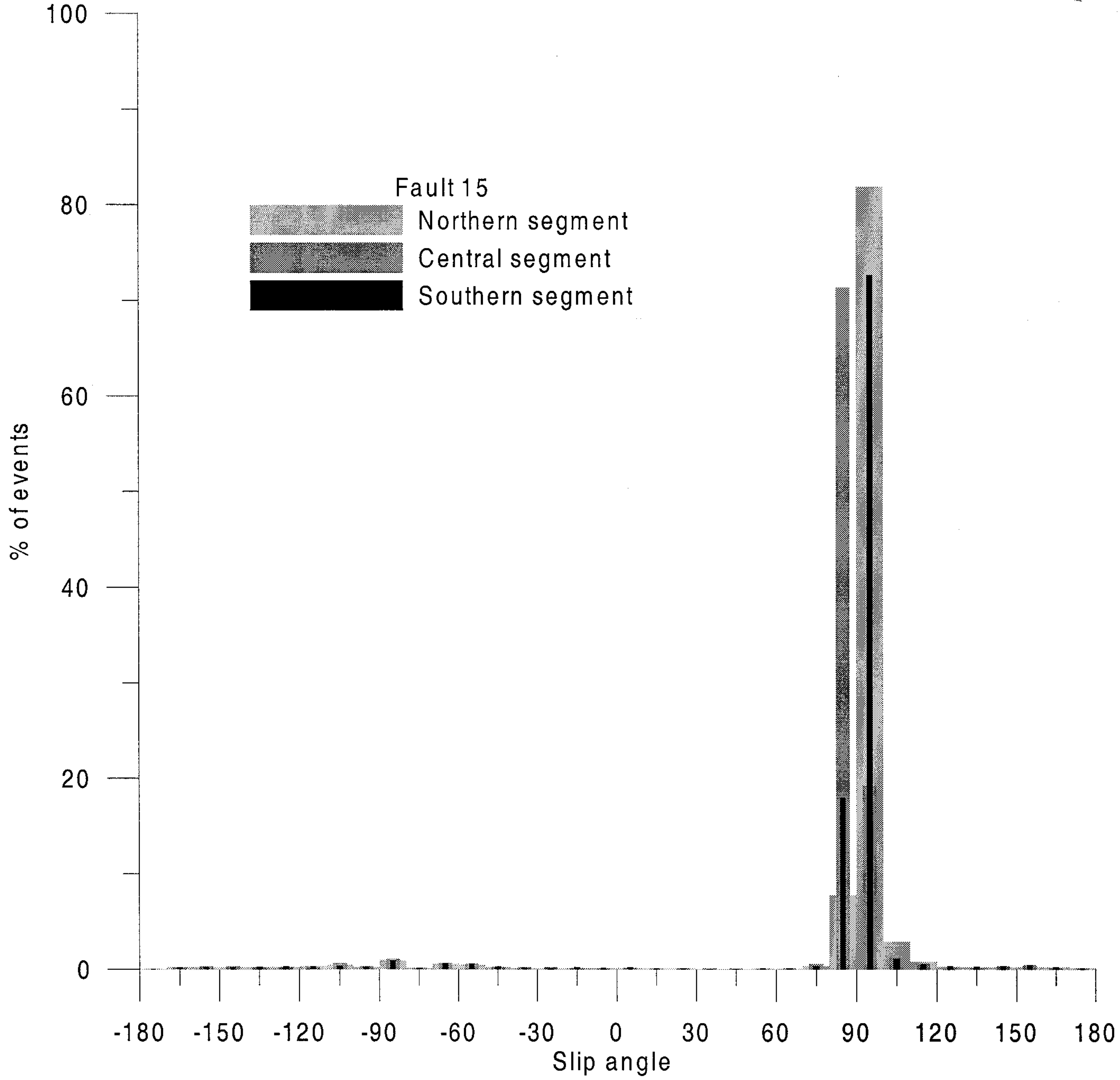
Fault 15
Northern segment
Central segment
Southern segment
% of events
100
80
60
40
20
0
-180
-150
-120
-90
-60
-30
0
30
60
90
120
150
180
Slip angle

Figure 19

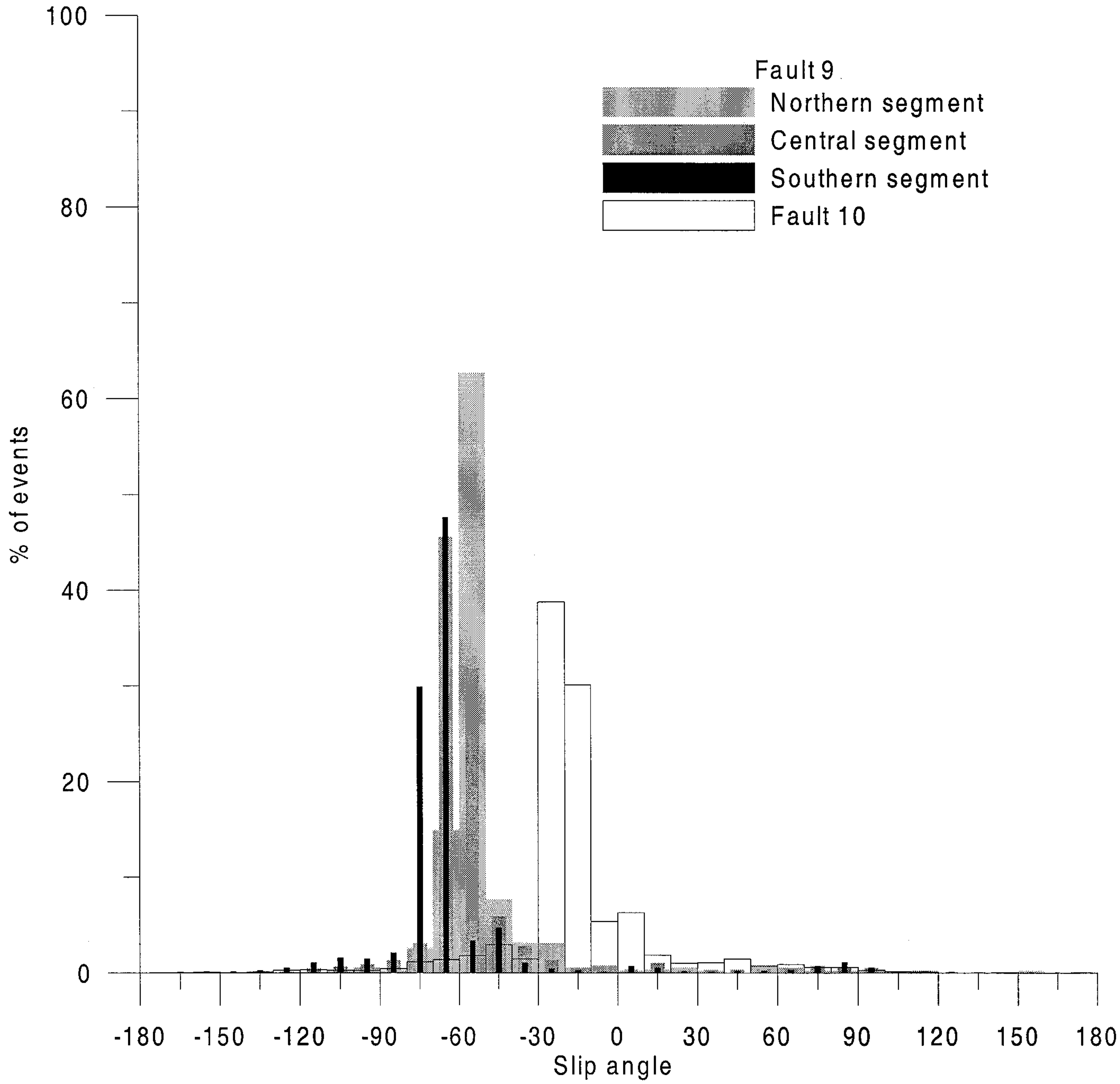

100
80
60
40
20
0
% of events
Fault 9
Northern segment
Central segment
Southern segment
Fault 10
-180
-150
-120
-90
-60
-30
0
30
60
90
120
150
180
Slip angle

Figure 20